Transverse Zeeman Effect of the Excitation Spectra of Boron and Thallium Impurities in Germanium*

H. P. Soepangkat† and P. Fisher
Department of Physics, Purdue University, West Lafayette, Indiana 47907
(Received 29 December 1972)

The results are presented of an experimental investigation of the transverse Zeeman effect (Voigt configuration) of the excitation spectra of boron and thallium impurities in germanium. These have been studied with the magnetic field $\vec{B}$ along ⟨100⟩, ⟨111⟩, or ⟨110⟩ using linearly polarized radiation. The results are compared with the calculations of Lin-Chung and Wallis and the theory of Bhattacharjee and Rodriguez. The g factors given by the former authors have permitted one case out of thirty-two possibilities to be selected for $\vec{B}\|\langle 100\rangle$. Consequently, the g factors of several of the states of both impurities have been found; this represents the first determination of the g factors for any of the group-III impurities in germanium. The values obtained for the principal g factors, $g'_{1/2}$ and $g'_{3/2}$, of the ground states are -1.53 ± 0.09 and 0.03 ± 0.04, respectively, for boron, and -1.4 ± 0.7 and 0.23 ± 0.04, respectively, for thallium. The values of $g^D_{1/2}$ and $g^D_{3/2}$, for example, the g factors of the excited state of the D line are -6.14 ± 0.13 and 0.07 ± 0.03, and -5.7 ± 0.2 and 0.06 ± 0.23, for boron and thallium, respectively. The difference in value between $g'_{3/2}$ of boron and thallium is taken to be due to the difference in ground-state wave functions of these two impurities, i.e., a manifestation of the chemical shift. The excited states have essentially the same g factors as is to be expected for effective-mass-like levels. The quadratic factors have not been determined separately for each state. The relative intensities of the D components for $\vec{B}\|\langle 100\rangle$ are in good agreement with theory. From the results obtained for $\vec{B}\|\langle 100\rangle$, it is possible to predict the linear splittings and relative intensities of the Zeeman components for $\vec{B}\|\langle 111\rangle$ and $\vec{B}\|\langle 110\rangle$. Good agreement is found with the experimental results for the D components under the latter orientation; the agreement is not as good for $\vec{B}\|\langle 111\rangle$. Some success is obtained in the interpretation of the C line for all three orientations if this is taken to be due mainly to an excitation to the Γ_7 state of the $\Gamma_7+\Gamma_8$ combination predicted by the effective-mass theory. The behavior of the G line has not been well understood.

I. INTRODUCTION

The energy states of groups-III and -V impurities in germanium and silicon have been investigated relatively extensively using spectroscopic techniques.[1] One of the objectives in this work has been to correlate the states accessible in such experiments with the predictions of effective-mass theory.[2] For the shallow donors, correspondence has been obtained to a high degree not only in the comparisons of binding energies of excited states[3-7] but also in their symmetries,[4,8,9] deformation-potential constants,[3,4,8-11] and Zeeman splittings.[12-19] Some success has also been obtained for group-III acceptors. In the case of germanium, the observed spectra[20] of all five group-III impurities agree well among themselves and correlate favorably with the results of effective-mass calculations.[21] For these impurities in silicon, the four which have been studied show some marked differences in their spectra[1,22] and do not vindicate the calculations[23,24] to the same extent as for germanium.

Piezospectroscopic studies have been made[22,25-27] for group-III acceptors in both silicon and germanium and some of the symmetries of the states and their deformation-potential constants determined. These latter observations, for the ground states, are in good agreement with those calculated[28,29] from the corresponding valence-band constants; these calculations are based on the effective-mass wave functions of the ground states. However, deformation-potential constants of the excited states have not yet been calculated, and hence a complete one-to-one comparison between the experimental results and theory cannot be made using the piezospectroscopic observations as basis.

The experimental studies made previously[15,30] of the Zeeman effect of group-III impurities in silicon and germanium were not very detailed. More recently some longitudinal Zeeman measurements have been made[31] for both silicon and germanium. For shallow acceptors in germanium, the original Zeeman measurements[30] did not employ polarized radiation, were not sufficiently detailed to provide systematic data, and were not carried out at high enough resolution for the magnetic fields used to resolve many of the Zeeman components. In addition, very little theoretical consideration had been given to the problem so that the experimental results were little understood. However, recently Lin-Chung and Wallis[32] have evaluated the g factors of a number of the states of group-III impurities in germanium. Also, they have calculated the intensities of the Zeeman components of a number of the excitation lines for

a magnetic field $\vec{B}$ parallel to a ⟨100⟩ crystallographic orientation. Hence an experimental investigation of the Zeeman effect of such spectra should afford the best opportunity for comparison between theory and experiment not for just the ground state but also for the excited states. In addition, an even more recent theoretical study has been made by Bhattacharjee and Rodriguez[33] of the Zeeman splittings and relative intensities of components not only for $\vec{B} \parallel \langle 100 \rangle$ but also for $\vec{B} \parallel \langle 111 \rangle$ and $\vec{B} \parallel \langle 110 \rangle$.

The present paper describes a detailed investigation of the transverse Zeeman effect (Voigt configuration) of the excitation spectra of boron and thallium impurities in germanium. Preliminary accounts of this work have appeared elsewhere.[34,35] These two particular group-III impurities were chosen for study since one, boron, has the smallest chemical shift of the shallow acceptors, and the other, thallium, has the largest.[20] Hence any effect that the chemical shift has on the ground-state g factors and the intensities of the Zeeman components should have the most likelihood of being revealed from a study of these two impurities.

II. EXPERIMENTAL APPARATUS AND PROCEDURES

The excitation spectra of neutral group-III acceptors in germanium occur in the energy range of about 6–16 meV. The far-infrared spectrometer[36] used for the observations incorporated a Perkin–Elmer model 210B[37] grating monochromator. The detector was an indium-doped germanium bolometer[38] cooled by a bath of liquid helium whose temperature was held at 1.68 °K. The bolometer was housed in a type CLF-3 metal cryostat[39] modified[36] in much the same way as described by Zwerdling *et al.*[40] The characteristics of the detector were very similar to those described in Ref. 40. The present detector gave a signal-to-noise (S/N) ratio of better than seven times larger than that of the Golay detector used in one of the earlier studies of such spectra.[20] The source consisted of the quartz capsule of an H-100-$A4/T$ mercury lamp[41] operated with dc, the infrared radiation being chopped at 260 Hz to give the maximum signal-to-noise ratio. Reststrahlen plates, ground aluminum reflectors, and transmission filters were used to eliminate undesired higher-order components from the diffracted radiation.[36] The monochromator was calibrated using the energies[42] of the pure rotational absorption lines of atmospheric water vapor. The radiation was plane polarized by a type 186[37] wire-grid polarizer on a polyethylene substrate.

A 4-in. Varian model 400[43] magnet, with its pole pieces tapered to $1\frac{1}{2}$-in.-diam faces, was used for the investigations. The magnet gap was set at $\sim\frac{9}{16}$ in., thus allowing magnetic fields of up to ~ 21 kG to be obtained. The sample cryostat was similar in design to one discussed elsewhere,[44] being modified to have a tail piece of square cross section of $\frac{1}{2}$-in. side with two pairs of rectangular ports, one above the other, which were sealed with wedged crystalline quartz windows. The entire cryostat could be lowered or raised to move the sample in or out of the beam and thus permit the transmission of the sample to be obtained.

The germanium samples were cut from single-crystal ingots which were oriented either by x rays or by an optical method.[45] The magnetic field was applied across the width of each sample and hence was transverse to the direction of propagation, $\vec{k}$, of the radiation. All samples were cut such that $\vec{k}$ was parallel to a ⟨110⟩ direction. The samples, when ground to their required dimensions, possessed a wedge in their thickness along their length sufficient to suppress interference fringes. Carborundum powders of mesh size Nos. 600, 1200, and 3200 were successively used to prepare the samples, followed by etching to obtain "highly reflective" surfaces. The orientations of the finished samples were checked by taking Laue photographs and found to be within 2° of those desired.

After leaving the sample cryostat, the radiation was collected by a series of "light pipes" which directed it onto the bolometer detector. The output of the detector was amplified by a phase-sensitive amplifier[46] and encoded as a function of photon energy in IBM cards by a procedure described by Onton.[47] The computer program used to analyze the data incorporated a smoothing procedure[48] and calculated the absorption coefficient at each point of observation.

III. THEORY

Several calculations have been reported on the Zeeman effect of shallow acceptors in germanium. Some of these have utilized either the effective-mass wave functions or the effective-mass formalism to obtain explicit values for g factors and intensities of the Zeeman components. The first such calculation is that of Bir *et al.*[28] in which the g factors of the acceptor ground state are expressed in terms of those of the free hole using Schechter's[23] effective-mass wave functions. Only the linear Zeeman effect is considered, the Zeeman Hamiltonian used being derived from symmetry arguments alone. The most general form of this Hamiltonian for the present problem was originally derived by Kleiner[49] and included the quadratic terms. The results of Bir *et al.* are given in Table I, where the g factors have been tabulated using two notations which are related; this is done for convenience in the discussion later. The second entry for Bir *et al.* in this

TABLE I. Calculated g factors for the ground state of group-III impurities in germanium.[a]

	g_1'	g_2'	$g_{1/2}'$	$g_{3/2}'$
Bir *et al.*[b]	5.66	−0.26	5.60	5.10
	5.89[c]	−0.18[c]	5.85	5.59
Suzuki *et al.*[d]	−1.44	0.56	−1.30	−0.19
	−0.91	0.56	−0.77	0.35
Lin-Chung and Wallis[e]	−1.13	0.63	−0.97	0.29

[a]The g factors are given using two notations, those of Refs. 28 and 29. This is done for convenience later. The relationships between these are $g_1' = g_{1/2}' - \frac{1}{8}(g_{3/2}' - g_{1/2}')$ and $g_2' = \frac{1}{2}(g_{3/2}' - g_{1/2}')$.

[b]See Ref. 28.

[c]Calculated from $g_1' = 0.86g_1 + 0.23g_2$ and $g_2' = -0.04g_1 + 0.78g_2$ given in Table 4 of Ref. 28 using the values of g_1 and g_2 reported in Ref. 50.

[d]See Ref. 29.

[e]See Ref. 32.

table is the values obtained by substituting the results of Hensel and Suzuki[50] for the free-hole g factors into the expressions of Bir *et al.* for g_1' and g_2'.

The above g factors have also been calculated by Suzuki *et al.*[29] They have used an effective-mass Zeeman Hamiltonian with effective-mass envelope wave functions, the latter being calculated by them using the valence-band parameters communicated by Hensel.[29] These results are included in Table I. In addition, they have recalculated the g factors using the same envelope functions but the band parameters of Stickler *et al.*[51] in the effective-mass Zeeman Hamiltonian. These results are also listed in Table I.

A calculation identical to that of Suzuki *et al.*,[29] but using the Mendelson–James[21] envelope functions, has been made by Lin-Chung and Wallis (LCW).[32] However, they have extended the calculations to give g factors for the excited acceptor states and intensities of the Zeeman components of the various excitation lines for $\vec{B} \parallel \langle 100 \rangle$. The g factors obtained for the ground state by LCW are given in Table I; those for the excited states are given in a later table.

It is seen that the results of Suzuki *et al.* and LCW are in good agreement. It is not clear why those of Bir *et al.* are so different, particularly since the results of their calculation for the deformation-potential constants of germanium are almost identical to those of Suzuki *et al.*

In the recent study of Bhattacharjee and Rodriguez (BR),[33] the exact Zeeman Hamiltonian of Kleiner[49] has been used to obtain expressions for the energies of the Zeeman sublevels for $\vec{B} \parallel \langle 100 \rangle$, $\langle 111 \rangle$, or $\langle 110 \rangle$, and relative intensities of the Zeeman components of an electric-dipole transition for these directions of $\vec{B}$. For either a Γ_6 or Γ_7 state the Zeeman Hamiltonian is given by

$$H_Z^{(i)} = \mu_B g_{(i)} \vec{B} \cdot \vec{J} + q_{(i)} B^2 , \tag{1}$$

where $i = 6$ or 7 corresponds to Γ_6 or Γ_7, the two $j = \frac{1}{2}$ irreducible representations of the double point group $\bar{T}_d$; μ_B is the Bohr magneton. For the Γ_8 ground state

$$H_Z^{(8)} = \mu_B g_1' \vec{B} \cdot \vec{J} + \mu_B g_2' (B_x J_x^3 + B_y J_y^3 + B_z J_z^3) + q_1' B^2 + q_2' (\vec{B} \cdot \vec{J})^2 + q_3' (B_x^2 J_x^2 + B_y^2 J_y^2 + B_z^2 J_z^2), \tag{2}$$

where $\vec{J}$ corresponds to an angular-momentum state with $j = \frac{3}{2}$. Identical expressions hold for Γ_8 excited states except that the g's and q's are different. These will be distinguished by a superscript that designates the excitation line connecting each with the ground state; for example, g_1^D and g_2^D will represent the g factors of the Γ_8 final state that is believed[20,26,27] to be associated with the D line.

It is shown[33] that with $\vec{B} \parallel \langle 100 \rangle$, for example, the energies of the Zeeman sublevels of Γ_6 or Γ_7 are

$$E_\mu^{(i)} = \mu_B g_{(i)} B\mu + q_{(i)} B^2 , \tag{3}$$

where $\mu = +\frac{1}{2}$ or $-\frac{1}{2}$, and for the ground state,

$$E_\mu^{(8)} = \mu_B (g_1' \mu + g_2' \mu^3) B + [q_1' + (q_2' + q_3')\mu^2] B^2, \tag{4}$$

where $\mu = \frac{3}{2}, \frac{1}{2}, -\frac{1}{2}$, or $-\frac{3}{2}$. Similar expressions hold for the excited Γ_8 states. The relationship between the two notations used for the g factors given in Table I is obtained by defining for the Γ_8 states what have been called the principal g factors,[34,35] viz.,

$$E_\mu - E_{-\mu} = 2\mu\mu_B g_{|\mu|}' B, \tag{5}$$

for the ground state and similarly for the excited states. Equation (5) gives

$$g_{1/2}' = g_1' + \tfrac{1}{4} g_2' , \qquad g_{3/2}' = g_1' + \tfrac{9}{4} g_2' , \tag{6}$$

which correspond to the quantities $g_{1/2}$ and $g_{3/2}$ defined in Refs. 29 and 32.

Similar but more complicated results have been obtained by BR for the energies of the Zeeman sublevels with $\vec{B} \parallel \langle 111 \rangle$ and $\vec{B} \parallel \langle 110 \rangle$. These are not presented here but will be used later in the interpretation of the experimental results.

In the group-theoretical treatment of BR, the relative intensities of the Zeeman components of a $\Gamma_8 \rightarrow \Gamma_8$ transition have been determined in terms of the parameters u and v of Rodriguez *et al.*,[52] where u and v are different for each such transition. Table II gives the relative intensities for electric-dipole transitions from a Γ_8 ground state with $\vec{B} \parallel \langle 100 \rangle$ in the Voigt configuration. In this table, $E_\parallel$ corresponds to the electric vector $\vec{E}$ of

TABLE II. Relative intensities of the Zeeman components in the Voigt configuration with $\vec{B} \parallel \langle 100 \rangle$ for electric-dipole transitions.[a]

Zero-field transition	$E_\parallel$ Component	$E_\parallel$ Relative intensity	$E_\perp$ Component	$E_\perp$ Relative intensity
$\Gamma_8 \rightarrow \Gamma_6$	$\pm\frac{1}{2} \rightarrow \pm\frac{1}{2}$	$\frac{1}{2}$	$\mp\frac{3}{2} \rightarrow \mp\frac{1}{2}$	$\frac{3}{8}$
			$\mp\frac{1}{2} \rightarrow \pm\frac{1}{2}$	$\frac{1}{8}$
$\Gamma_8 \rightarrow \Gamma_7$	$\pm\frac{3}{2} \rightarrow \mp\frac{1}{2}$	$\frac{1}{2}$	$\pm\frac{3}{2} \rightarrow \pm\frac{1}{2}$	$\frac{1}{8}$
			$\pm\frac{1}{2} \rightarrow \mp\frac{1}{2}$	$\frac{3}{8}$
$\Gamma_8 \rightarrow \Gamma_8$	$\pm\frac{3}{2} \rightarrow \mp\frac{1}{2}$	$\frac{1}{4}-\frac{1}{2}v$	$\pm\frac{3}{2} \rightarrow \pm\frac{1}{2}$	$\frac{1}{4}-(\frac{3}{16})u+\frac{1}{4}v$
			$\pm\frac{1}{2} \rightarrow \mp\frac{1}{2}$	$(\frac{3}{16})u$
	$\pm\frac{1}{2} \rightarrow \mp\frac{3}{2}$	$\frac{1}{4}+\frac{1}{2}v$	$\mp\frac{1}{2} \rightarrow \mp\frac{3}{2}$	$\frac{1}{4}-(\frac{3}{16})u-\frac{1}{4}v$
			$\mp\frac{3}{2} \rightarrow \pm\frac{3}{2}$	$(\frac{3}{16})u$

[a]See Ref. 32.

the incoming radiation parallel to $\vec{B}$, while $E_\perp$ is for $\vec{E} \perp \vec{B}$. Similar results have been obtained by BR for $\vec{B} \parallel \langle 111 \rangle$ and $\vec{B} \parallel \langle 110 \rangle$, but again, these are more complicated, and are not presented here.

A comparison between the calculated intensities of LCW and the relative intensities of Table II enables values of the different u's and v's to be estimated.[53] It is found for the D and G lines that $u_D \simeq \frac{1}{6}$, $v_D \simeq \pm\frac{3}{8}$, $u_G \simeq \frac{8}{9}$, and $v_G \simeq \pm\frac{1}{3}$. It should be noted that the above values for u_D and v_D appear to be consistent with the piezospectroscopic results of Ref. 26 for thallium impurity in germanium. A calculation of the intensities for the stress-induced D components has been made by Dickey and Dimmock[27] for a uniaxial force along $\langle 100 \rangle$. A comparison of their results (Table I, Ref. 27) and those of Rodriguez *et al.*[52] (Table XV) gives $u_D = -\frac{2}{27}$, which is inconsistent with symmetry.

IV. EXPERIMENTAL RESULTS

A. Zero Magnetic Field

The excitation spectrum of boron impurity in germanium without external perturbation is shown in Fig. 1; a sample different from that used for the rest of the spectrum was used to obtain the G line. A similar spectrum for thallium impurity is given in Fig. 2. The resolution bars indicated on these figures are the geometrical spectral slit widths of the spectrometer. These spectra are to be compared with the appropriate ones of Ref. 20. The present result for boron impurity was ob-

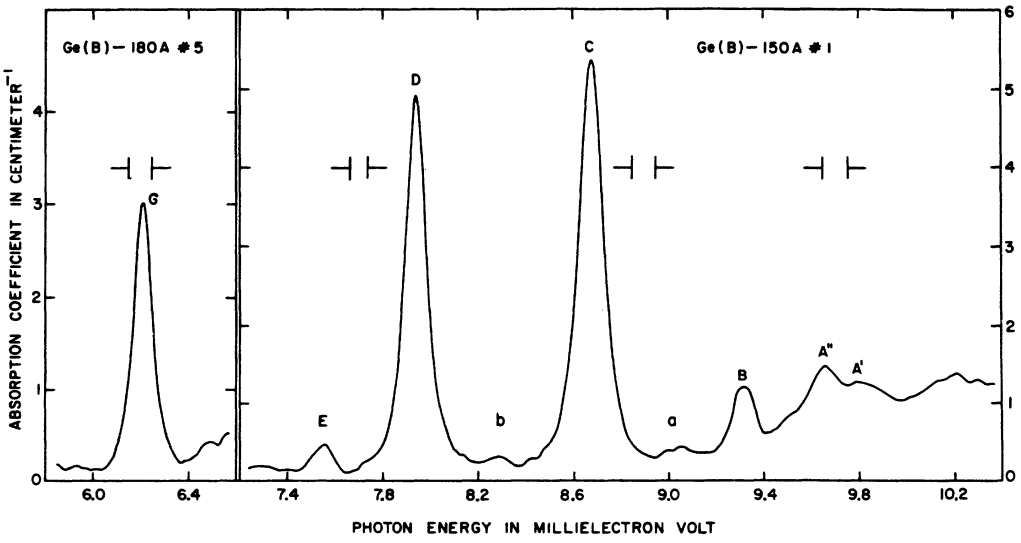

FIG. 1. Excitation spectrum of boron impurity in germanium. The acceptor concentration N_A of sample Ge(B) – 150A No. 1 was $\sim 2 \times 10^{14}$ cm^{-3} while that of Ge(B) – 180A No. 5 was $\sim 8 \times 10^{14}$ cm^{-3}. Liquid helium used as coolant.

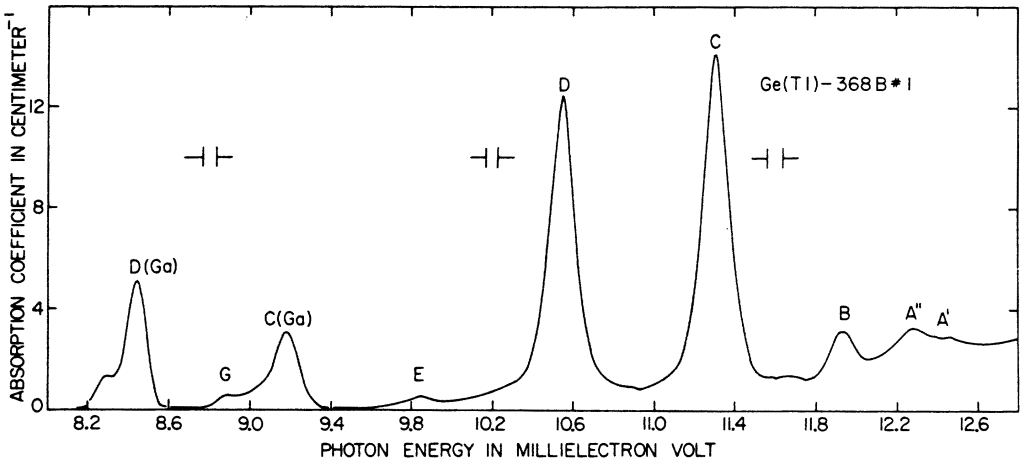

FIG. 2. Excitation spectrum of thallium impurity in germanium; $N_A \simeq 2 \times 10^{14}$ cm^{-3}. Liquid helium used as coolant.

tained with about the same resolution as that of Fig. 1 in Ref. 20, but with a S/N ratio that was about twice as large. The spectrum in Fig. 2 was taken with about the same S/N ratio but with twice the resolution of the results given in Ref. 20.

For the present results, the higher-energy lines A', A'', and B are not as well defined as those of Ref. 20 even though the resolution is as good or better. Since the cryostat used in the present case was expected to be less effective in cooling the sample, these differences are believed to be due to higher sample temperatures than those achieved previously. In Fig. 1, it is seen that the intensity of the C line is larger than that of the D line in contradiction to the results given in Ref. 20, Fig. 1. It is felt that the present results are more reliable, in view of the superior detector used. In Fig. 2, the lines labeled C(Ga) and D(Ga) are believed to be due to contamination of the thallium ingot with gallium.[20] In the present case, these are stronger relative to the G line than in the spectrum of Fig. 5, Ref. 20; this appears to confirm the assumption that these are due to gallium since two different samples cut from different ingots were used in the two instances. The origin of the shoulder on the low-energy side of D(Ga) in Fig. 2 is unknown.

Only boron and thallium impurities have been studied since the ground states of these correspond to the two extremes of the chemical shift[20] of the group-III impurities. Table III shows the energies of the various transitions and their energy spacings relative to the D line. The energies shown for the C and D lines have been obtained by taking the means of the results of a number of observations of these lines; the errors shown span all values used in each case. The remaining lines were observed only once, the errors being estimates of the experimental errors. The position of the E line of thallium may be doubtful since it occurs at an energy close to that of the B line of gallium which, as is seen above, is a serious contaminant in the present sample.

B. Zeeman Effect

The following gives a description of the results of the transverse Zeeman effect (Voigt configuration) for the above excitation spectra. For each orientation of $\vec{B}$, the light propagation vector $\vec{k}$ is along a ⟨110⟩ direction.

1. $\vec{B} \parallel \langle 100 \rangle$

a. Boron impurity. The Zeeman effect of the excitation spectrum of boron impurity in germanium for $\vec{B} \parallel \langle 100 \rangle$ is shown for several magnitudes of applied field in Figs. 3 and 4, for $E_\parallel$ (electric vector of radiation, $\vec{E}$, parallel to $\vec{B}$) and $E_\perp$ ($\vec{E} \perp \vec{B}$). Two samples of different boron concentration were used in obtaining these spectra. Since

TABLE III. Energies of transitions observed for boron and thallium impurities in germanium. Units are meV.

Transition	Boron	Thallium
A'	9.79 ± 0.03	12.42 ± 0.07
A''	9.66 ± 0.02	12.29 ± 0.03
B	9.33 ± 0.02	11.93 ± 0.01
C	8.681 ± 0.003[a]	11.30 ± 0.01
D	7.936 ± 0.003[a]	10.552 ± 0.007
E	7.55 ± 0.03	9.86 ± 0.04
G	6.21 ± 0.01	8.91 ± 0.03

[a]The errors for the C and D lines of boron impurity in germanium span all values of a number of observations of these lines. The errors for all the other lines are estimates of the experimental error.

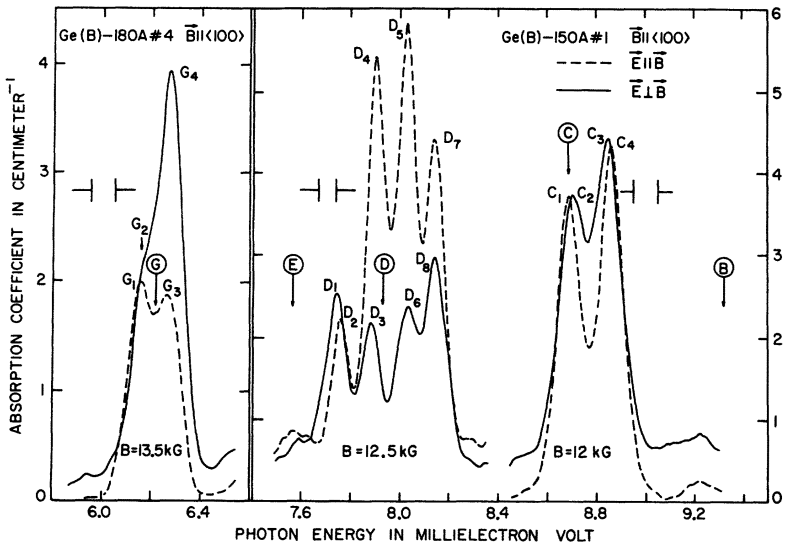

FIG. 3. Zeeman effect of the excitation spectrum of boron impurity in germanium for $\vec{B} \parallel \langle 100 \rangle$ at the magnetic fields indicated. For Ge(B) − 180A No. 4, $N_A \simeq 7 \times 10^{14}$ cm^{-3}. The encircled labels and associated arrows designate the positions of the lines at zero magnetic field. Liquid helium used as coolant.

the G line is substantially weaker than either the C or D lines[20] it was necessary to use a higher impurity concentration in order to obtain well-defined Zeeman components of the former. The B line, which is also weaker than the C and D lines, is not as readily accessible since it is much more susceptible to both concentration and thermal broadening than the G line and it is also much less isolated from other lines of the spectrum.

Figure 5 shows the dependence of the energies of the Zeeman components on $|\vec{B}|$ for both $E_{\parallel}$ and $E_{\perp}$ for the lines B, C, D, E, and G. The B components were not well defined particularly at the higher fields (see Figs. 3 and 4), thus giving rise to some scatter in their estimated positions; there appears to be at least one component for each polarization. As can be seen, the B and E lines were studied over a larger range of fields than were C, D, and G. This was done in an attempt to establish unambiguously the origin of all the components at higher fields. It was not practical to study the C, D, or G lines at the lower fields since their Zeeman components were unresolved below certain values of $|\vec{B}|$. The C line gives rise to four distinct components C_1, C_2, C_3, and C_4, where the two extreme components are of different polarization to that of the two intermediate components. It might be noted that C_1 and C_2 have been resolved only because of their different polarizations; this is also the case for C_3 and C_4. For the D line, four well-resolved components are seen for each polarization giving a total of eight possible components although D_7 and D_8 may have the same energy. Only one E component is seen while there are four G components. In the latter case, there are two for each direction of polarization.

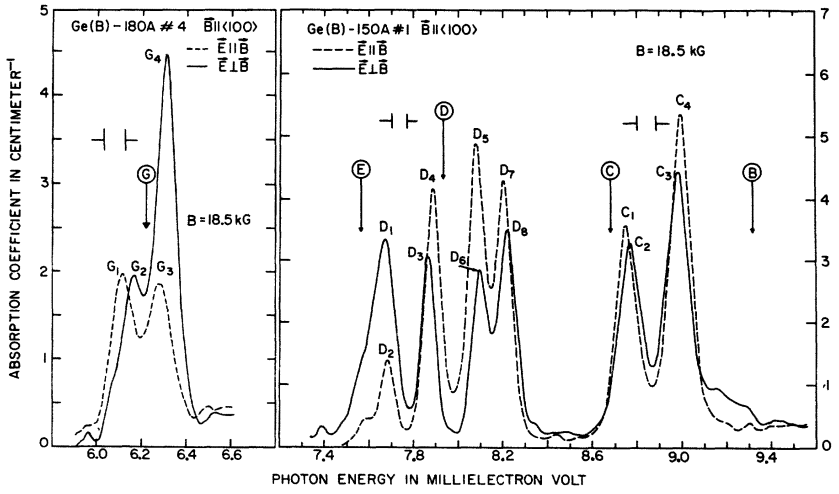

FIG. 4. Same as Fig. 3 but for $|\vec{B}| = 18.5$ kG.

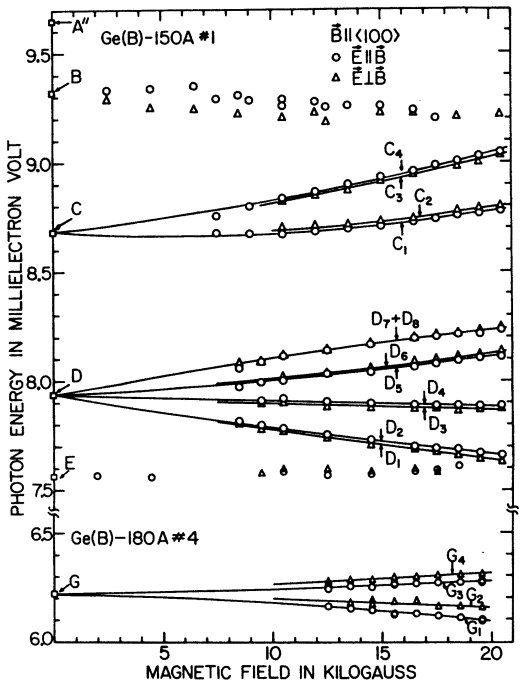

FIG. 5. Dependence of the energies of the Zeeman components on $|\vec{B}|$ for boron impurity in germanium with $\vec{B} \parallel \langle 100 \rangle$.

The fits shown to the various components in Fig. 5 represent the results of linear least-squares fits to $[\epsilon_X(|\vec{B}|) - \epsilon_X(0)]/|\vec{B}|$ vs $|\vec{B}|$, where ϵ_X is the energy of the Xth transition. This representation of the data for the D components is shown in

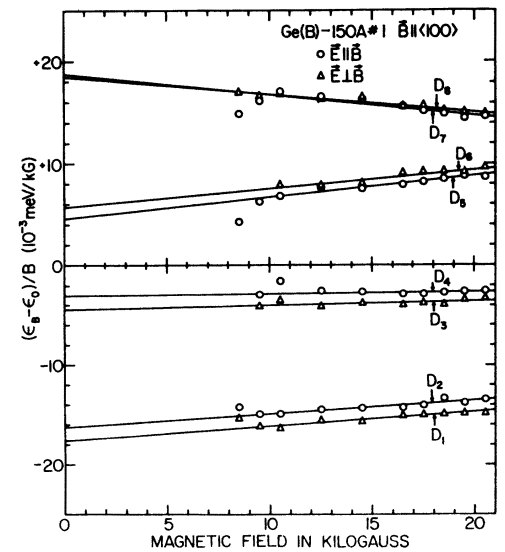

FIG. 6. Linear least-squares fits of the Zeeman D-component data to $[\epsilon_X(|\vec{B}|) - \epsilon_X(0)]/|\vec{B}|$ vs $|\vec{B}|$ for boron impurity in germanium, where ϵ_X is the energy of the Xth transition; $\vec{B} \parallel \langle 100 \rangle$.

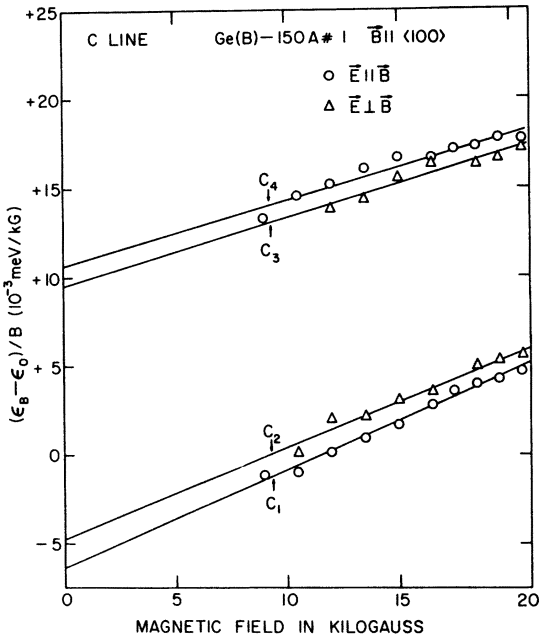

FIG. 7. Same as Fig. 6 but for the C components.

Fig. 6, and for the C and G components in Figs. 7 and 8, respectively. The results obtained are given in Table IV, where the coefficients a and b are defined by $\epsilon_X(|\vec{B}|) = \epsilon_X(0) + aB + bB^2$. The errors shown are the most probable errors resulting from the least-squares fits. It should be noted that

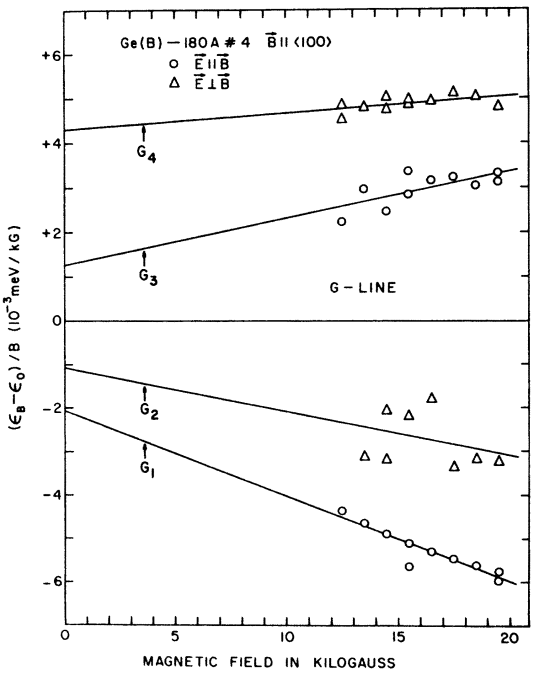

FIG. 8. Same as Fig. 6 but for the G components.

TABLE IV. Energies of the C, D, and G Zeeman components of boron impurity in germanium with $\vec{B} \parallel \langle 100 \rangle$.[a,b]

Component	a (meV/kG) $\times 10^2$	b (meV/kG^2) $\times 10^4$
C_1	-0.636 ± 0.022	$+5.51 \pm 0.14$
C_2	-0.475 ± 0.041	$+5.15 \pm 0.20$
C_3	$+0.949 \pm 0.053$	$+3.78 \pm 0.32$
C_4	$+1.065 \pm 0.035$	$+3.66 \pm 0.22$
D_1	-1.763 ± 0.018	$+1.47 \pm 0.11$
D_2	-1.628 ± 0.020	$+1.38 \pm 0.13$
D_3	-0.447 ± 0.029	$+0.46 \pm 0.18$
D_4	-0.301 ± 0.017	$+0.21 \pm 0.11$
D_5	$+0.456 \pm 0.024$	$+2.13 \pm 0.15$
D_6	$+0.570 \pm 0.036$	$+1.87 \pm 0.22$
D_7	$+1.871 \pm 0.037$	-1.96 ± 0.23
D_8	$+1.849 \pm 0.017$	-1.72 ± 0.22
G_1	-0.208 ± 0.032	-1.96 ± 0.19
G_2	-0.11 ± 0.12	-1.00 ± 0.75
G_3	$+0.128 \pm 0.043$	$+1.04 \pm 0.26$
G_4	$+0.430 \pm 0.021$	$+0.38 \pm 0.14$

[a]The coefficients a and b are defined by $\epsilon(B) = \epsilon(0) + aB + bB^2$ (see text).

[b]The errors indicated are the most probable errors obtained from the linear least-squares fits (see text).

in making the fits, those few data points which occur at the smallest fields and obviously lie well away from the straight lines have been omitted.

b. Thallium impurity. In Fig. 9 is shown the Zeeman effect for the C and D lines of thallium impurity in germanium at $|\vec{B}| = 18.5$ kG and $\vec{B} \parallel \langle 100 \rangle$. The labeling of the components follows that of Figs. 3 and 4. The dependence of the energies of the components on $|\vec{B}|$ is shown in Fig. 10.

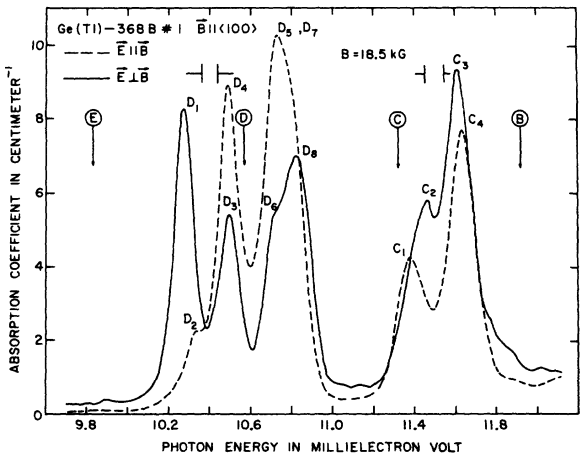

FIG. 9. Zeeman effect of the excitation spectrum of thallium impurity in germanium for $\vec{B} \parallel \langle 100 \rangle$ and $|\vec{B}| = 18.5$ kG. $N_A \simeq 2 \times 10^{14}$ cm^{-3}. The encircled labels and associated arrows designate the positions of the lines at zero magnetic field. Liquid helium used as coolant.

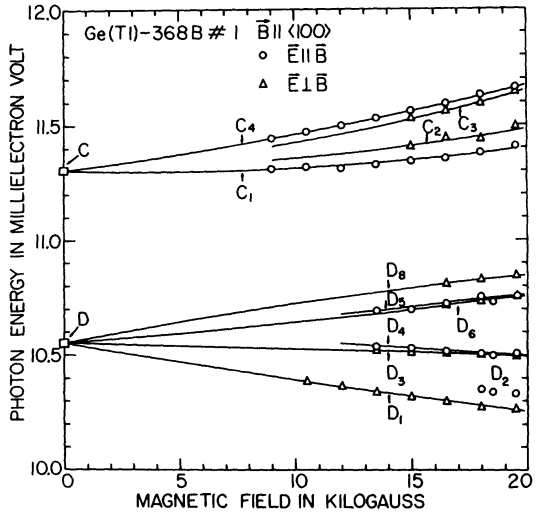

FIG. 10. Dependence of the energies of the C and D Zeeman components on $|\vec{B}|$ for thallium impurity in germanium with $\vec{B} \parallel \langle 100 \rangle$.

The full curves in this figure have been drawn in the same manner as those in Fig. 5. The linear fits to the data in the case of thallium are given in Figs. 11 and 12 and summarized in Table V.

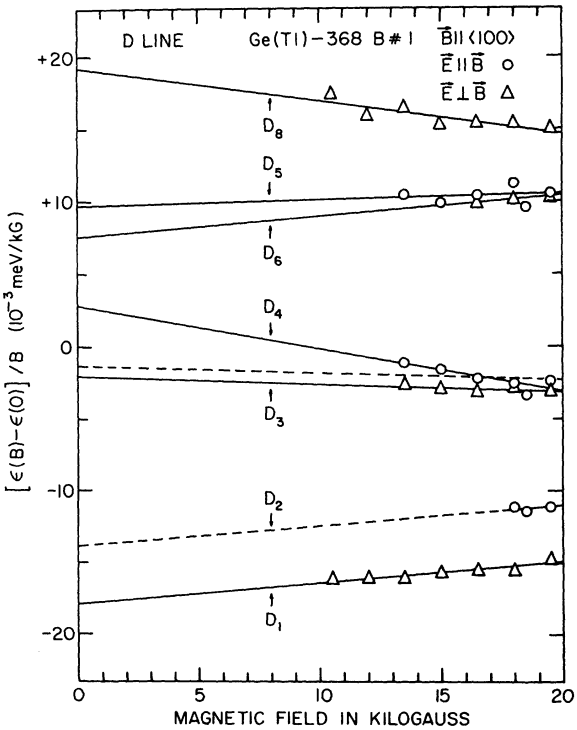

FIG. 11. Linear least-squares fits of the Zeeman D-component data to $[\epsilon_X(|\vec{B}|) - \epsilon_X(0)]/|\vec{B}|$ vs $|\vec{B}|$ for thallium impurity in germanium, where ϵ_X is the energy of the Xth transition; $B \parallel \langle 100 \rangle$.

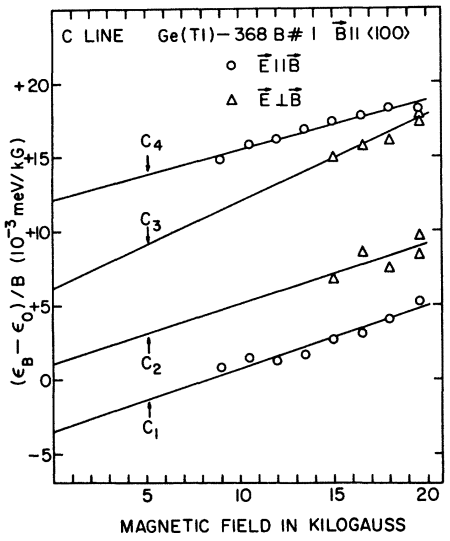

FIG. 12. Same as Fig. 11 but for the C components.

The dashed line drawn through the data for D_2 and parallel to the line through D_1 has been used to obtain the values of a and b given in Table V for D_2; this will be discussed later. The meaning of the dashed line drawn through the data points of D_4 parallel to the line fitted to the data of D_3 will also be discussed later.

2. $\vec{B} \parallel \langle 111 \rangle$

The Zeeman effect for the C, D, and G lines of boron impurity, at several values of $|\vec{B}|$ and with $\vec{B} \parallel \langle 111 \rangle$, is shown in Figs. 13 and 14. The spectrum of thallium impurity has not been examined for this direction of $\vec{B}$. The dependence of the energies of the Zeeman components on $|\vec{B}|$ is given in Fig. 15. Again, four C components are observed, two for each polarization. However, the width of C_1 is such as to suggest that this may be composed of more than one component. The D line exhibits six components, three for each polarization, although it is not clear if D_3 and D_4 are different transitions; similarly for D_5 and D_6. Also D_1 is broader than D_2, suggesting that it may consist of two or more unresolved components. For the G line there appear to be four components, two for each direction of polarization, two of these,

TABLE V. Energies of the C and D Zeeman components of thallium impurity in germanium with $\vec{B} \parallel \langle 100 \rangle$.[a]

Component	a (meV/kG) $\times 10^2$	b (meV/kG^2) $\times 10^4$
C_1	-0.347 ± 0.063	$+4.21 \pm 0.43$
C_2	$+0.10 \pm 0.27$	$+4.0 \pm 1.5$
C_3	$+0.62 \pm 0.12$	$+5.78 \pm 0.73$
C_4	$+1.234 \pm 0.022$	$+3.23 \pm 0.18$
D_1	-1.774 ± 0.027	$+1.41 \pm 0.09$
D_2	-1.38 ± 0.03[b]	$+1.41 \pm 0.09$[b]
D_3	-0.212 ± 0.038	-0.48 ± 0.23
D_4	$+0.28 \pm 0.11$	-2.95 ± 0.63
D_5	$+0.97 \pm 0.14$	$+0.40 \pm 0.85$
D_6	$+0.68 \pm 0.11$	$+1.70 \pm 0.60$
D_7	...	...
D_8	$+1.925 \pm 0.061$	-2.27 ± 0.39

[a]The coefficients a and b are defined by $\epsilon(B) = \epsilon(0) + aB + bB^2$ (see text); the errors given are the most probable errors obtained from the least-squares fits.

[b]These values have been obtained by assuming that b for D_2 is the same as that for D_1 and fitting the data points for D_2 to a straight line with this slope. The value for a is the mean value of all such a's; the error given spans the range of these a's (see text).

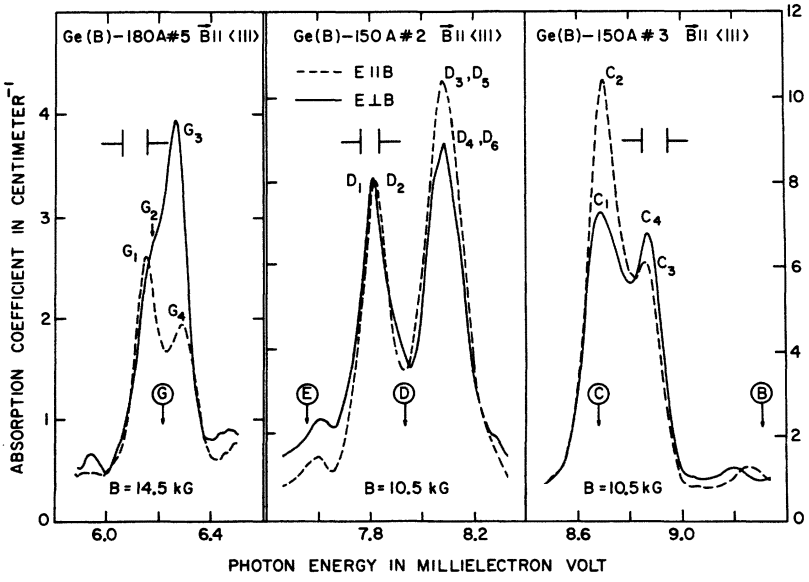

FIG. 13. Zeeman effect of the excitation spectrum of boron impurity in germanium for $\vec{B} \parallel \langle 111 \rangle$. $|\vec{B}|$ is 14.5 kG for the G line and 10.5 kG for the rest. Acceptor concentrations of samples Ge(B) − 150A No. 2, Ge(B) − 150A No. 3, and Ge(B) − 180A No. 5 were $\sim 4 \times 10^{14}$ cm^{-3}, $\sim 2.5 \times 10^{14}$ cm^{-3}, and $\sim 8 \times 10^{14}$ cm^{-3}, respectively. The encircled labels and associated arrows designate the positions of the lines at zero magnetic field. Liquid helium used as coolant.

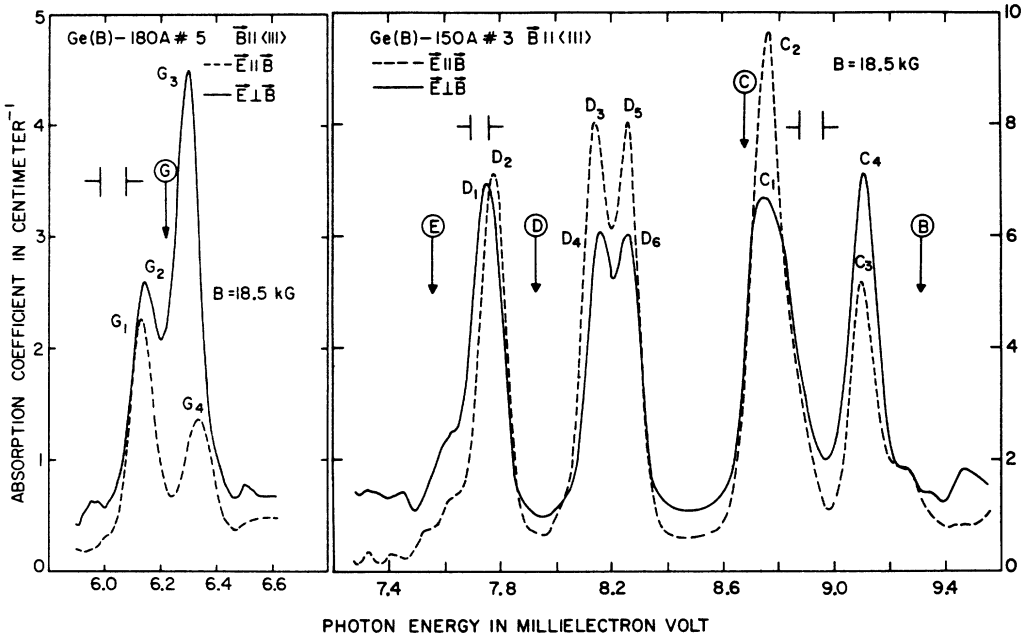

FIG. 14. Same as Fig. 13 but for $|\vec{B}| = 18.5$ kG.

viz., G_1 and G_2, are very close in energy. As before, the full curves fitted to the data points are the results of linear least-squares fits. The manner in which these fits were obtained may be understood from Figs. 16–18. The parameters a and b for each component are given in Table VI. The fittings for the C and G components (Figs. 17 and 18) were obtained in a straightforward way. However, because D_3 and D_5 were not resolved except at the largest fields only a few data points were obtained for them. A linear least-squares fit to

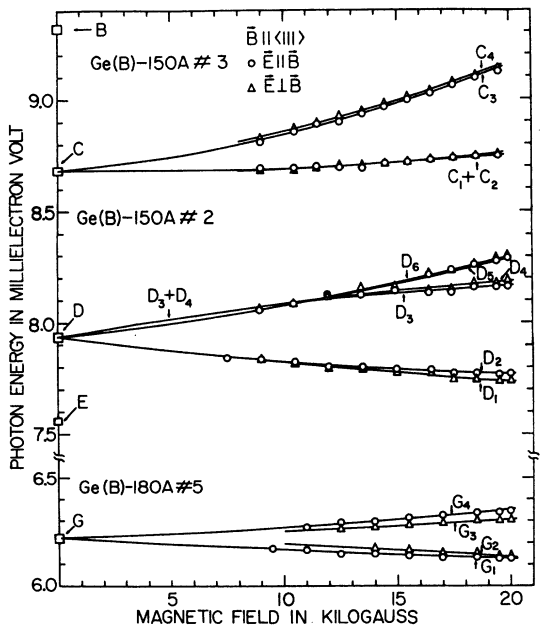

FIG. 15. Dependence of the energies of the Zeeman components on $|\vec{B}|$ for boron impurity in germanium with $\vec{B} \parallel \langle 111 \rangle$.

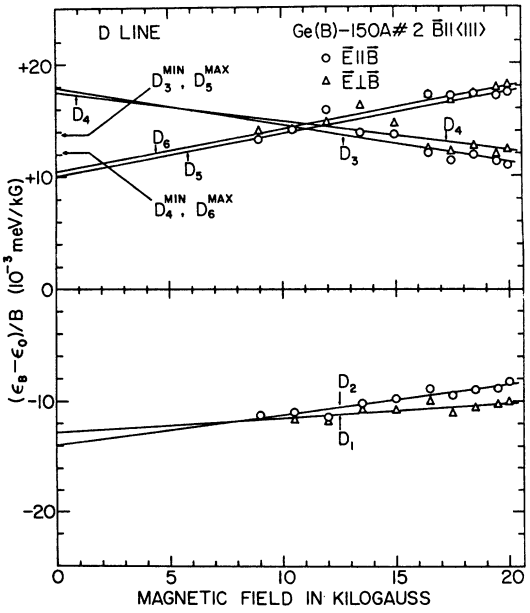

FIG. 16. Linear least-squares fits of the Zeeman D-component data to $[\epsilon_X(|\vec{B}|) - \epsilon_X(0)]/|\vec{B}|$ vs $|\vec{B}|$ for boron impurity in germanium, where ϵ_X is the energy of the Xth transition; $\vec{B} \parallel \langle 111 \rangle$.

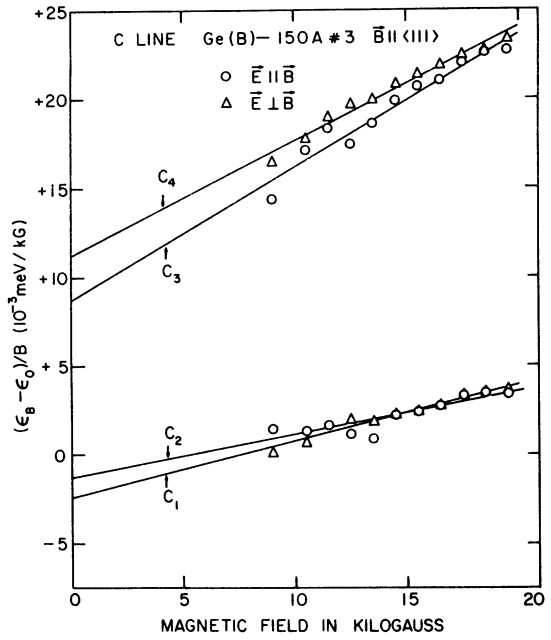

FIG. 17. Same as Fig. 16 but for the C components.

these few points can give unreliable values and hence the results obtained in this way were not used. The same applies to D_4 and D_6. The straight line in Fig. 16 through the data points for D_3, for example, represents a fit to the various D_3 components as well as to the unresolved components D_3, D_5 observed at lower fields (see, for example, Fig. 13). This fit will give an intercept which will be larger than the true one. The values for D_3, D_5 were also used in making the fit to D_5, hence this fit will give an intercept which will be smaller than the true one. The intercept at $(13.8 \pm 0.2) \times 10^{-3}$ meV/kG, indicated by D_3^{MIN}, D_5^{MAX} in Fig. 16, was obtained by fitting to the D_3, D_5 components only. A fit such as this should give an intercept that will correspond to the minimum value that this quantity can have for D_3 and the maximum value for D_5. A similar procedure was followed for D_4 and D_6. In this case, the intercept at $(12.18 \pm 0.14) \times 10^{-3}$ meV/kG, indicated by D_4^{MIN}, D_6^{MAX} in Fig. 16, has the same meaning as for D_3, D_5. The values of a and b listed in Table VI are those taken from the straight lines in Fig. 16.

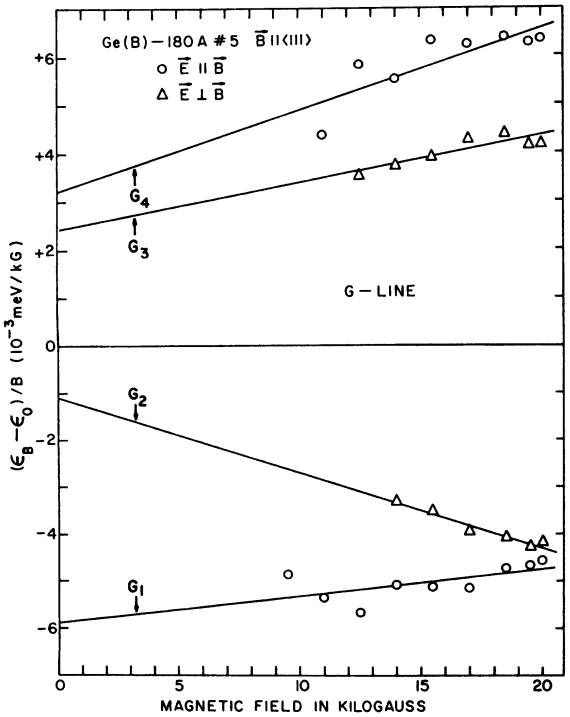

FIG. 18. Same as Fig. 16 but for the G components.

TABLE VI. Energies of the C, D, and G Zeeman components of boron impurity in germanium with $\vec{B} \parallel \langle 111 \rangle$.[a,b]

Component	a (meV/kG) $\times 10^2$	b (meV/kG^2) $\times 10^4$
C_1	-0.246 ± 0.025	$+3.22 \pm 0.17$
C_2	-0.137 ± 0.045	$+2.47 \pm 0.31$
C_3	$+0.873 \pm 0.063$	$+7.46 \pm 0.43$
C_4	$+1.123 \pm 0.032$	$+6.42 \pm 0.22$
D_1	-1.278 ± 0.039	$+1.30 \pm 0.25$
D_2	-1.394 ± 0.034	$+2.74 \pm 0.22$
D_3	$+1.785 \pm 0.093$	-3.31 ± 0.60
D_4	$+1.749 \pm 0.099$	-2.60 ± 0.63
D_5	$+1.003 \pm 0.095$	$+3.71 \pm 0.61$
D_6	$+1.041 \pm 0.059$	$+3.73 \pm 0.37$
G_1	-0.590 ± 0.029	$+0.58 \pm 0.18$
G_2	-0.155 ± 0.032	-1.59 ± 0.13
G_3	$+0.243 \pm 0.027$	$+0.95 \pm 0.16$
G_4	$+0.322 \pm 0.054$	$+1.67 \pm 0.33$

[a]The coefficients a and b are defined by $\epsilon(B) = \epsilon(0) + aB + bB^2$ (see text).

[b]The errors indicated are the most probable errors obtained from linear least-squares fits (see text).

3. $\vec{B} \parallel \langle 110 \rangle$

For $\vec{B} \parallel \langle 110 \rangle$, the relative intensities of the Zeeman components depend upon the direction of the light propagation vector $\vec{k}$.[33] Only one direction of $\vec{k}$ has been used in the present measurements. The results for $\vec{B} \parallel [110]$ and $\vec{k} \parallel [1\bar{1}0]$ are shown in Figs. 19 and 20 for boron impurity. In Fig. 19, the D components were observed with $|\vec{B}| = 13.0$ kG, while for the C components, $|\vec{B}| = 11.5$ kG. In Fig. 20, $|\vec{B}| = 18.5$ kG for both sets of components. The G line was not studied at all in this case while the C line was only examined at a few fields. There are again four C components, however, all these are broader than in the cases for $\vec{B} \parallel \langle 100 \rangle$ and $\vec{B} \parallel \langle 111 \rangle$. It is not clear if this is

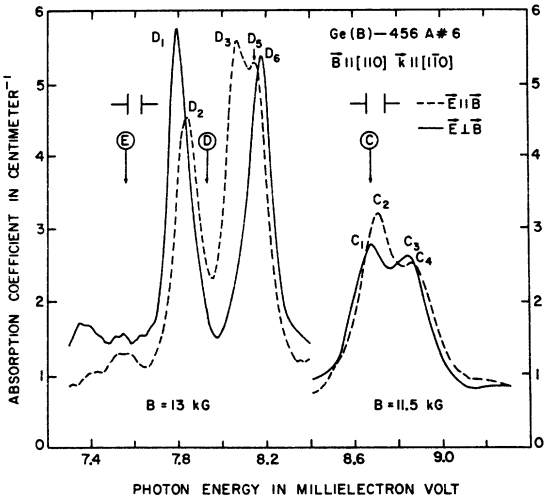

FIG. 19. Zeeman effect of the excitation spectrum of boron impurity in germanium for $\vec{B} \parallel [110]$ at the magnetic fields indicated, with $\vec{k} \parallel [1\bar{1}0]$. $N_A \simeq 4 \times 10^{14}$ cm^{-3}. The encircled labels and associated arrows designate the positions of the lines at zero magnetic field. Liquid helium used as coolant.

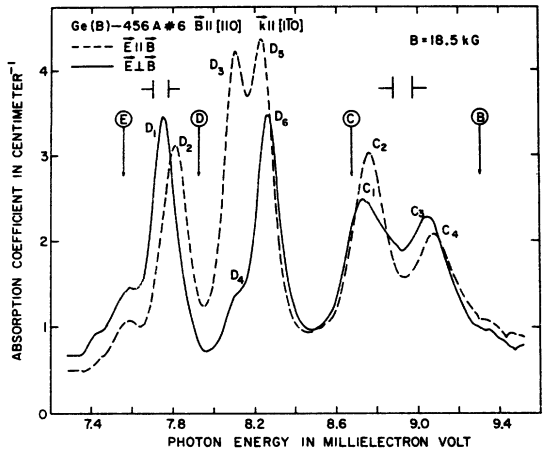

FIG. 20. Same as Fig. 19 but for $|\vec{B}| = 18.5$ kG.

due to concentration broadening, temperature broadening, or whether each is composed of several components. Figure 21 is a plot of ϵ_X vs $|\vec{B}|$ for the D components. Six such components are observed, D_4 emerging only at the highest fields. The fits to the data in Fig. 21 were obtained from the results of the least-squares fits of Fig. 22; the numerical values for these are listed in Table VII. The excitation spectrum of thallium impurity has not been examined for this direction of applied $\vec{B}$.

V. DISCUSSION

A. $\vec{B} \parallel \langle 100 \rangle$

It is clear from the calculated splittings and relative intensities[33] that the case of $\vec{B} \parallel \langle 100 \rangle$ is by far the simplest, thus we will discuss the results for this orientation first. In order to obtain the g factors for the various energy states, it is necessary to correlate the observed Zeeman components with explicit transitions. The interpretation of the D line will be considered first since this has proved to be the most tractable. The interpretation of the results[26,27] of piezospectroscopic studies shows that the D line is in all probability due to a $\Gamma_8 \rightarrow \Gamma_8$ transition.[20] Thus the relative intensities of the Zeeman components in Figs. 3 and 4 should correspond to those given in Table II.

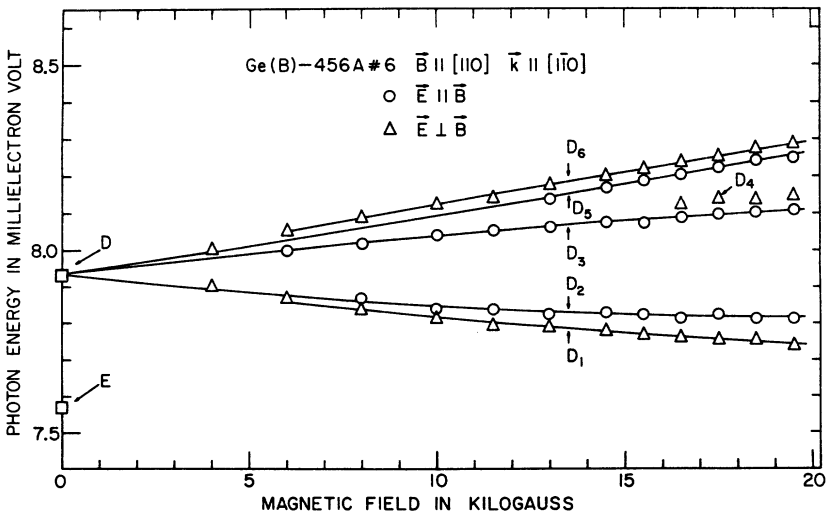

FIG. 21. Dependence of the energies of the Zeeman D components on $|\vec{B}|$ for boron impurity in germanium with $\vec{B} \parallel [110]$ and $\vec{k} \parallel [1\bar{1}0]$.

Hence, for $E_{\parallel}$, four components are expected. All four of these will be of equal intensity only if $v_D = 0$, otherwise they will group into two pairs in each of which the two components have equal intensity. It is clear from Figs. 3 and 4 that $v_D \neq 0$ since all the D components are not of equal intensity for $E_{\parallel}$. The magnitude of v_D can be obtained by comparing the intensities of the different components. For all values of $|\vec{B}|$ used, it was found that D_4 and D_5 were about equal in intensity and larger than D_2 and D_7. Since D_5 and D_7 are less resolved than are D_2 and D_4 it was more meaningful to compare the intensities of the latter in order to find $|v_D|$. It was estimated that the ratio of the intensities of D_4 and D_2 is ~3 corresponding to $|v_D| \simeq 0.25$, which is to be compared with the theoretical value of $|v_D| \simeq \frac{3}{8}$ given earlier. This latter value of $|v_D|$ predicts that the intensity of D_4 should be seven times that of D_2; this is obviously incorrect. Since there are only four D components for $E_{\perp}$ and these are not of equal intensity, it is clear from Table II that $u_D \simeq 0$ thus confirming qualitatively the calculations of LCW. The two outer $E_{\perp}$ components, D_1 and D_8, appear to be of equal intensity while the two weaker inner components, D_3 and D_6, are also of about equal intensity. Taking $u_D = 0$ and $|v_D| = 0.25$ and using the results of Table II, it is estimated that the relative intensity of D_1 to D_3 and D_8 to D_6 should be ~1.7. This is somewhat larger than appears to be the case experimentally, as may be seen from Figs. 3 and 4. If u_D is made nonzero, this ratio becomes larger than 1.7. A value of $|v_D| = 0.2$ and u_D still zero gives a value of 1.5 for the above intensity ratio; this is more realistic. However, it has been pointed out by BR that if $u = 0$ then v is also zero. Hence, since $v_D \neq 0$, u_D must be somewhat different from zero.

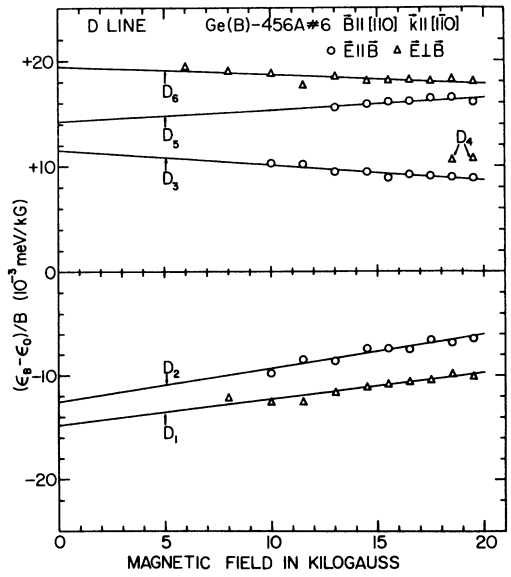

FIG. 22. Linear least-squares fits of the Zeeman D-component data to $[\epsilon_X(|\vec{B}|) - \epsilon_X(0)]/|\vec{B}|$ vs $|\vec{B}|$ for boron impurity in germanium, where ϵ_X is the energy of the Xth transition; $\vec{B} \parallel [110]$ and $\vec{k} \parallel [1\bar{1}0]$.

TABLE VII. Energies of the D Zeeman components of boron impurity in germanium with $\vec{B} \parallel [110]$ and $\vec{k} \parallel [1\bar{1}0]$.[a,b]

Component	a (meV/kG) $\times 10^2$	b (meV/kG^2) $\times 10^4$
D_1	-1.475 ± 0.031	$+2.46 \pm 0.21$
D_2	-1.259 ± 0.042	$+3.26 \pm 0.27$
D_3	$+1.155 \pm 0.025$	-1.43 ± 0.16
D_4	•••	•••
D_5	$+1.424 \pm 0.047$	$+1.12 \pm 0.28$
D_6	$+1.950 \pm 0.027$	-0.85 ± 0.19

[a]The coefficients a and b are defined by $\epsilon(B) = \epsilon(0) + aB + bB^2$ (see text).

[b]The errors indicated are the most probable errors obtained from the linear least-squares fits.

The assumption that the four transitions of strength $\frac{3}{16}u$ are essentially of zero intensity produces an interesting consequence, viz., coupling via electric-dipole transitions only occurs between $\frac{1}{2}$ states and $\frac{3}{2}$ states (see Table II). Thus, in obtaining an interpretation of the spectra, the allowed transitions of the type $\frac{3}{2} \rightarrow \frac{1}{2}$ can be considered independent of those of the type $\frac{1}{2} \rightarrow \frac{3}{2}$. Since the sign of v_D is undetermined at this point it is necessary to consider two cases, viz., either $v_D > 0$ or $v_D < 0$. Each of these gives 16 different ways in which the data can be interpreted. Many other cases have been rejected on the basis of the energies of the components being incompatible with the data.[54] A further reduction in the number of possible cases is obtained if the signs of the $g_{1/2}$ factors are taken to be the same as those calculated by LCW. It is felt that these should be at least reliable in their sign since they are large in magnitude compared to the calculated $g_{3/2}$ factors.[32] With these restrictions, the 16 cases for each sign of v_D are reduced to four. If, in addition, the relative magnitudes of the $g_{1/2}$'s and $g_{3/2}$'s given by LCW are assumed to be correct, then only one case remains corresponding to a positive value for v_D. This surviving case, for the linear effects alone, is illustrated in Fig. 23. The g factors deduced using this result are given in Table VIII along with those calculated by LCW. The results are again given using the two previous notations. The ratios $p' = g_1'/g_2'$ and $p^D = g_1^D/g_2^D$ of BR are also included in the table. Note that the present notation for these ratios is slightly different from that of BR. The numerical values of the g factors were obtained by subtracting the a values of Table IV corresponding to the pairs of lines defining a given

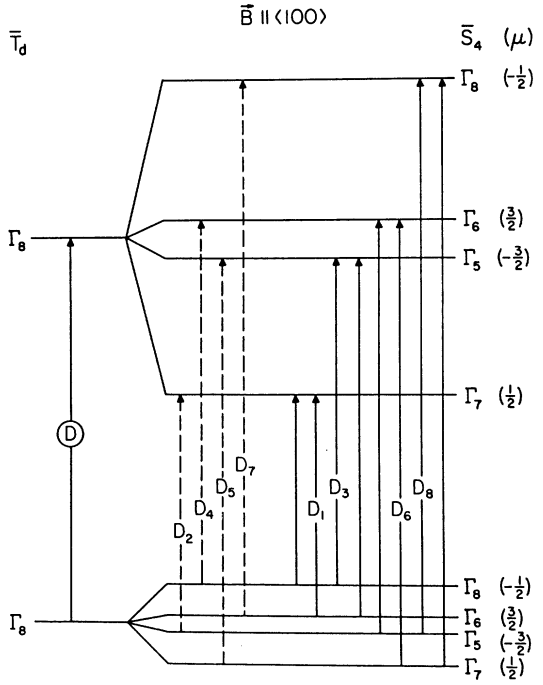

FIG. 23. Energy-level and electric-dipole transition scheme for the Zeeman D components of boron in germanium with $\vec{B} \parallel \langle 100 \rangle$. The unlabeled transitions were not observed.

level splitting and using Eq. (5). In each case, as may be seen from Fig. 23, each splitting is given by two such pairs; the average values of the splittings were used to obtain the g factors. The errors given in Table VIII are due to either the most probable errors listed in Table IV or the difference between the average value of $E_\mu - E_{-\mu}$ and each $E_\mu - E_{-\mu}$ estimated from the a's of the latter table, whichever is larger. It should be mentioned that the values given for the p's in Table VIII have been estimated from the ratios of the expressions for g_1 and g_2 (see footnote to Table I) rather than directly from the values of g_1 and g_2 given in the table. In this way it can be seen that the error in g_1 is not independent of that of g_2 (as was assumed by BR) since each depends upon $g_{1/2}$ and $g_{3/2}$.

It might be noted that the g values obtained are consistent with the fact that no noticeable depopulation effects are observed. Such effects would be most pronounced for the components D_4 and D_5 or D_3 and D_6 (see Fig. 23). However, from Figs. 3 and 4, it is clear that the relative intensities of the components in each of the above pairs are little affected even when the ground-state splitting is increased by ~ 50%.

The above method for evaluating the g factors may not be without pitfalls. In the analysis it is assumed that the experimental situation conforms to the theoretical case of BR, viz., that there are no mixing effects between adjacent levels. If this were the case, the quadratic shift of the sublevels of the same $|\mu|$ would be the same within a given multiplet of levels. The observation that D_7 and D_8 have negative values of b while for the remaining components b is positive (see Table IV) implies that the $\mu = -\frac{1}{2}$ excited state has experienced some repulsions by, for example, the nearby complex level which is believed to be the final state of the C line.[20,26] The fact that D_7 and D_8 are behaving in a manner different from that expected from Eqs. (4) and (5) may be appreciated directly from Fig. 6. A comparison of the transitions given in Fig. 23 with the results shown in Fig. 6 shows that the splittings of the $\mu = \pm\frac{3}{2}$ levels for both the ground and excited states are obtained by subtracting D_1 from D_2, D_3 from D_4, etc., where in each case the pairs of components involved are represented by essentially parallel lines in Fig. 6; thus the quadratic effects cancel very closely in agreement with Eq. (5). However, the splittings of the $|\mu| = \frac{1}{2}$ levels are obtained by subtracting components represented in Fig. 6 by lines that are not parallel and hence some residual quadratic effect remains, in contradiction to Eq. (5). This effect is clearly most serious for the splitting of the excited $|\mu| = \frac{1}{2}$ states since this is obtained by subtracting D_1 from D_7 and D_2 from D_8. Thus the value of $g^D_{1/2}$ given in Table VIII may be somewhat in error. If

TABLE VIII. g factors for boron and thallium impurities in germanium from data for $\vec{B} \parallel \langle 100 \rangle$.[a,b]

	Boron	Thallium	Calculated[c]
g_1'	-1.73 ± 0.11	-1.57 ± 0.78	-1.13
g_2'	0.78 ± 0.07	0.80 ± 0.36	0.63
$g_{1/2}'$	-1.53 ± 0.09	-1.4 ± 0.7	-0.97
$g_{3/2}'$	0.03 ± 0.04[d]	0.23 ± 0.04[d]	0.29
g_1^D	-6.92 ± 0.16	-6.43 ± 0.21	-4.11
g_2^D	3.11 ± 0.08	2.89 ± 0.20	1.79
$g_{1/2}^D$	-6.14 ± 0.13	-5.7 ± 0.2	-3.66
$g_{3/2}^D$	0.07 ± 0.03	0.06 ± 0.23	-0.08
$g_{(1)}^C$	2.70 ± 0.13	1.81 ± 0.41	2.00
p'	-2.21 ± 0.06	$-1.97^{+0.12}_{-0.28}$	-1.79
p^D	-2.23 ± 0.01	-2.23 ± 0.08	-2.30

[a]Somewhat different values are obtained if certain assumptions are made; this is discussed in the text.

[b]The quantity $g_{(1)}^C$ is the same as $g_{1/2}^C$ of Ref. 32, while $p \equiv g_1/g_2$ of Ref. 33.

[c]See Ref. 30. Note that the results for the G line in this reference give $p^G = -2.10$.

[d]The interpretation of the data for the C line also yields a value for $g_{3/2}'$; this is discussed in the text.

it is assumed that only the $-\frac{1}{2}$ level of the excited state is undergoing repulsion then $g^D_{1/2}$ may be recalculated by considering the spacing given by $[\epsilon_D(0)-\epsilon_{D_1}(B)]+[\epsilon_D(0)-\epsilon_{D_2}(B)]$ and using only the linear effects. Such a calculation gives $g^D_{1/2} = -5.86\pm0.06$ with corresponding values of g^D_1 and g^D_2 of -6.60 ± 0.07 and $+2.97\pm0.05$, respectively[55]; however, the value of p^D is unchanged. The results for the ground state should not be affected while this approach cannot be used for $g^D_{3/2}$ since the two states involved may be affected by similar amounts.

It should be noted that if mixing does occur then the intensities of the transitions to mixed states will no longer conform to the results of Table II. This may well explain why the intensity of D_7 appears to be larger than that of D_2 in Figs. 3 and 4. However, it is not immediately obvious, without a detailed calculation of this effect, why D_8 should not be similarly affected.

From the existing data, it is not possible to determine the individual q's even without mixing. However, it is possible to evaluate combinations of these. Provided mixing effects are ignored, it is found from Eq. (4) and the values of b given in Table IV that

$$\left|[q^D_1+\tfrac{9}{4}(q^D_2+q^D_3)]\pm[q'_1+\tfrac{1}{4}(q'_2+q'_3)]\right| = (1.2\pm0.2)\times10^{-4}\,\text{meV/kG}^2$$

and

$$\left|[q^D_1+\tfrac{1}{4}(q^D_2+q^D_3)]\pm[q'_1+\tfrac{9}{4}(q'_2+q'_3)]\right| = (0.2\pm0.2)\times10^{-4}\,\text{meV/kG}^2.$$

From the above information it is possible to estimate the energies at which the four components of equal intensity $\frac{3}{16}u$ should occur for $E_\perp$. Of these, the highest-energy component should form a high-energy shoulder to D_8, while that of lowest energy should be a low-energy shoulder to D_1. The two intermediate components should occur at the minimum between D_3 and D_6. There is some asymmetry to D_1, part of which is due to an E component. The remainder may be attributed to the above lowest-energy component. If this is true, it is estimated that $u_D \sim 0.1$; however, it is believed that the error in this could be almost as large as the value itself.

The result for thallium impurity for $\vec{B}\parallel\langle100\rangle$ (see Fig. 9) is very similar to that of boron except that the various Zeeman components of the former are not as well separated as those of the latter. This is true for both the C and D components. The similarities are quite striking for the D components when a comparison is made between Figs. 6 and 11, or the results given in Tables IV and V; only the D_4 components show different behavior. The behavior of D_1, D_6, and D_8 for each impurity is practically identical, while that of D_3 and D_5 is very similar. This strongly suggests that the behavior of D_2 of thallium relative to D_1 should be the same as the relative behavior of these two components for boron. The data for D_2, resolved from D_4 only at higher fields, supports this suggestion. Hence, it has been assumed that this is the case and the dashed line through the data points of D_2 in Fig. 11 has been drawn parallel to that of D_1. The intercept obtained for D_2, which gives the value of a for this component in Table V, represents the average of the values obtained when the data of D_2 is fitted to a line of the same slope as that for D_1. Using the same scheme as that portrayed in Fig. 23 for boron, and the same procedures, the parameters of Table V give the g values for the ground state and the excited state of the D line for thallium that are listed in Table VIII.

If we follow the procedure discussed above to minimize the effect of mixing and use only the D_1 and D_2 components to obtain $g^D_{1/2}$, then a value of -5.5 ± 0.1 is obtained for this quantity. If it is assumed that the D_4 component should show the same relation to the D_3 component in both Figs. 6 and 11 then the dashed line through the data for D_4 in Fig. 11 is obtained.[56] The intercept of this dashed line has been determined in the same manner as was used for D_2 and is $a(D_4) = -0.00138 \pm 0.00051$ meV/kG, where the mean absolute error is given; also $b(D_4) = b(D_3) = -0.48\pm0.23$ meV/kG^2 (see Table V). If this value of $a(D_4)$ is used instead of that given in Table V, then $g'_{1/2} = -1.73 \pm 0.30$ and $g^D_{3/2} = -0.06\pm0.10$. Another alternative may be used to determine $g'_{1/2}$ and that is to ignore D_4 and simply use D_5 and D_3; in this case $g'_{1/2} = -2.04\pm0.30$.

Finally, for the D line of thallium, it is found that $v_D \sim \frac{1}{4}$. This value is obtained by comparing the intensities of the D_1, D_2, D_3, and D_4 components.

The C line for both boron and thallium for $\vec{B}\parallel\langle100\rangle$ exhibits a relatively simple Zeeman pattern. It might be expected that a pattern of great complexity should occur since the C line could be due to transitions to a $\Gamma_7+\Gamma_8$ combination. However, if it is assumed that only the $\Gamma_8-\Gamma_7$ transition is observed, then a straightforward interpretation can be obtained as far as the g factors are concerned. This interpretation assumes that the ordering and splitting of the Zeeman sublevels in the ground state is that determined by the interpretation of the D lines. In order that the observed energy spacings of the C components conform to the g factors of the ground state, the g factor of the Γ_7 excited state of the C line must be positive. This gives the scheme shown in Fig. 24. The values of $g^C_{(7)}$ ($\equiv g^C_{1/2}$) given in Table VIII for boron and

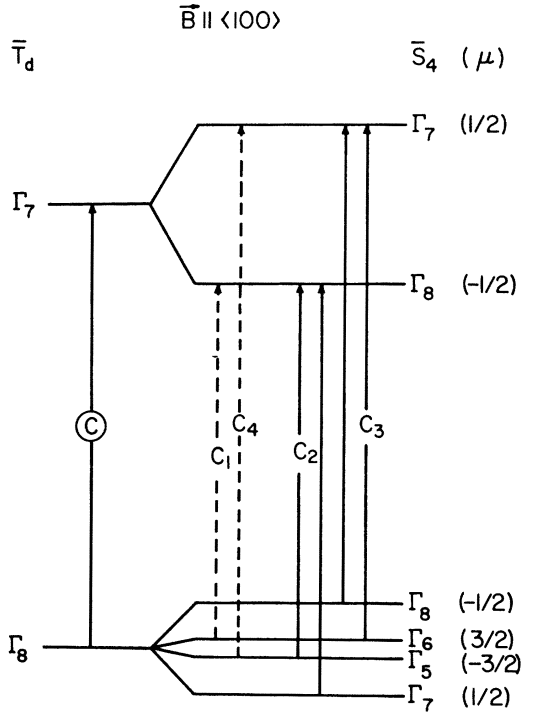

FIG. 24. Energy-level and electric-dipole transition scheme for the Zeeman C components of boron in germanium with $\vec{B} \parallel \langle 100 \rangle$ assuming a $\Gamma_8 \rightarrow \Gamma_7$ transition.

thallium have been deduced from this figure and the data of Tables IV and V. Values have also been obtained for $g'_{3/2}$ for these impurities. These are 0.08 ± 0.04 and 0.31 ± 0.14 for boron and thallium, respectively, which are to be compared with the values obtained above from the D line, viz., 0.03 ± 0.04 and 0.23 ± 0.04, respectively. Hence, if the present interpretation of the C line is correct this fixes the sign of $g'_{3/2}$ for boron. However, it is clear that there is a serious discrepancy between the scheme of Fig. 24, the data of Figs. 3 and 4, and the relative intensities given in Table II. The two transitions, $\pm\frac{1}{2} \rightarrow \mp\frac{1}{2}$, for $E_\perp$ which are not observed are predicted to be three times as intense as the two that are observed. This effect, if real, may be a consequence of the mixing of states, resulting in a large change in relative intensities without greatly affecting the value of $g^C_{(7)}$, not an unreasonable result. We have not attempted to determine the combination of q factors associated with the C components. However, if the interpretation illustrated in Fig. 24 is correct, then, according to Eqs. (3) and (4), all four C components should exhibit the same quadratic shift. Hence in the plots of Figs. 7 and 12 all four straight lines should be parallel. This is borne out fairly well for boron (Fig. 7) and also for C_1, C_2, and C_4 of thallium (Fig. 12). This suggests that the data for C_3 of thallium should be fitted to a straight line parallel to C_4, for example. When this is done a value of $a(C_3) \simeq 1.0 \times 10^{-2}$ meV/kG is found. Using this value for C_3 and proceeding as above, it is found that, for thallium, $g^C_{(7)} = 2.14$ and $g'_{3/2} = 0.20$; this latter value is in much better agreement with the value obtained from the D line (see Table VIII) than that given above.

The G line (studied only for boron) exhibits a rather unusual Zeeman pattern as may be appreciated from Figs. 3 and 4. While the components for $E_\parallel$ are fairly symmetrically disposed about the position of the unperturbed line in both energy and intensity, those for $E_\perp$ have a remarkable asymmetry in their intensities. In addition, the total splitting of the components is relatively small compared to that of the D line (see either Fig. 5 or Figs. 6 and 8). This latter aspect is a little surprising since LCW's calculation predicts that the splitting of the excited state of the G line should be nearly as large as that of the final state of the D line. If a direct comparison is made between the results given by BR and the present experimental results, very little agreement is obtained for $E_\perp$. In the case of $E_\parallel$, two strong and two weak components of equal intensity are predicted corresponding to the value of $|v_G| \simeq \frac{1}{3}$ given earlier. Ignoring quadratic effects these should be symmetrically disposed about the original G line. Six components of equal intensity are predicted for $E_\perp$ (each substantially weaker than the strong $E_\parallel$ components) corresponding to the value of $u_G \simeq \frac{8}{9}$ mentioned previously. Also, two very weak components are predicted. In order that a component as intense as G_4 (see Figs. 3 and 4) could occur, several of the stronger $E_\perp$ components would need to coincide in energy. This does not appear to be compatible with the scheme of LCW. It is possible to have four of the stronger $E_\perp$ components coincide in energy if the g factors of the excited state are equal in magnitude but opposite in sign to those of the ground state, contrary to the results of LCW. However, the energy of this resultant component would be the same as that of the original G line if only linear effects are considered. A qualitative agreement with the observed Zeeman pattern can be obtained if the quadratic shifts of the various sublevels are related in a specific way. Several cases are possible, depending upon the sign of v_G and, for example, the sign of the quadratic shift of the $\pm\frac{3}{2}$ sublevels of the excited state. If both of these are chosen to be positive, the following requirements must be satisfied. First, the quadratic shifts of the $\pm\frac{3}{2}$ excited state sublevels should be of the same sign and somewhat smaller than those of the $\pm\frac{1}{2}$ ground-state sublevels; second, the quadratic shifts of the $\pm\frac{3}{2}$ ground-state sublevels should be negative,

smaller in magnitude than those of the $\pm\frac{1}{2}$ excited state sublevels, and be repelled by the latter; and finally, the difference between the quadratic shifts of the two pairs of $\pm\frac{1}{2}$ sublevels should be equal to the sum of the shifts of the two pairs of $\pm\frac{3}{2}$ sublevels. It might be noted that in support of this conjecture the quadratic effects for the G line become significant at much lower fields than is the case for the D line (see Table IV). In addition, the value of $g'_{3/2}$ obtained from this model is close to that deduced from the C and D lines. However, the value of $g'_{1/2}$ so obtained is several times smaller than it should be. This represents a major difficulty with the model along with the fact that the signs of $g^G_{3/2}$ and $g^G_{1/2}$ are opposite to those of LCW.

An attempt has been made to correlate the experimental results for the G line with the predictions of either a $\Gamma_8 \rightarrow \Gamma_6$ or a $\Gamma_8 \rightarrow \Gamma_7$ transition.[33] This was not successful, but only linear effects were considered. However, in view of the correlation given in Ref. 20, it does not seem possible for the final state of the G line to be a twofold degenerate level.

B. $\vec{B} \parallel \langle 110 \rangle$

Provided we restrict ourselves to only the linear Zeeman effect, the interpretation given above for $\vec{B} \parallel \langle 100 \rangle$ determines the parameters which govern the intensities of the Zeeman components and the splitting of the energy states for both $\vec{B} \parallel \langle 110 \rangle$ and $\vec{B} \parallel \langle 111 \rangle$. This is clear from the results given by BR. Although only the D line has been studied in detail for $\vec{B} \parallel \langle 110 \rangle$, we will discuss this orientation first since its interpretation has proved to be relatively straightforward compared to that for $\vec{B} \parallel \langle 111 \rangle$. For the D line of boron impurity an interesting simplification occurs since both p' and p^D are almost equal to $-\frac{9}{4}$ (see Table VIII). This is a consequence of $g'_{1/2}$ and $g^D_{1/2}$ being large and $g'_{3/2}$ and $g^D_{3/2}$ being almost zero. If these latter two g factors were zero, then p' and p^D would be exactly $-\frac{9}{4}$ [see Eqs. (6)]; this will be called the *idealized case*.

From Eqs. (54) and (56) of BR, the linear splitting of the Γ_8 ground state is predicted to be

$$E'_{\pm 1/2} = \pm 0.911 \mu_B B g'_2 ,$$
$$E'_{\pm 3/2} = \pm 0.411 \mu_B B g'_2 , \qquad (7)$$

with identical expressions for the Γ_8 excited state of the D line except g'_2 is replaced by g^D_2. Thus, in the idealized case, the signs and magnitudes of g'_2 and g^D_2 determine the splitting of the ground and excited state, respectively. If the value of p' given in Table VIII is used, the numerical coefficients in Eqs. (7) become 0.891 and 0.431, respectively; for the excited state the differences are smaller. The energy scheme given in Fig. 25 has been drawn to conform to the idealized case exemplified by Eqs. (7), noting that the ratio of g^D_2 to g'_2 lies very close to 4 (see Table VIII). The relative intensities of the transitions have been calculated from the results of Tables XIV A and XIV C and Eqs. (55) and (77)–(82) of BR. These are summarized in Table IX; values of 0.1 and 0.2 have been used for u_D and v_D, respectively. The weak transitions in Table IX have been omitted from Fig. 25. The predictions contained in Fig. 25 and Table IX are combined in Fig. 26. A comparison between the predictions of Fig. 26 and the experimental results of Figs. 19 and 20 show good agreement if all the components in Fig. 26 are shifted to the right relative to the original D line. This comparison strongly suggests that the component labeled D_3 is composed of the two components D'_3 and D''_3. The D_4 component, not resolved from D_6 at the lower fields, is observed at the higher field of Fig. 20. The relative intensities of the components in this latter figure are substantially different from those in Fig. 19. This is believed to verify the prediction[33] that, in the case for $\vec{B} \parallel \langle 110 \rangle$, the quadratic terms in the Zeeman Hamiltonian give rise to relative intensities that are functions of $|\vec{B}|$. It should be noted that if a value of $v_D = -0.2$ is used, the intensities of the transitions $\pm\frac{3}{2} \rightarrow \pm\frac{1}{2}$ and $\pm\frac{1}{2} \rightarrow \pm\frac{3}{2}$ for $E_\parallel$ interchange; this

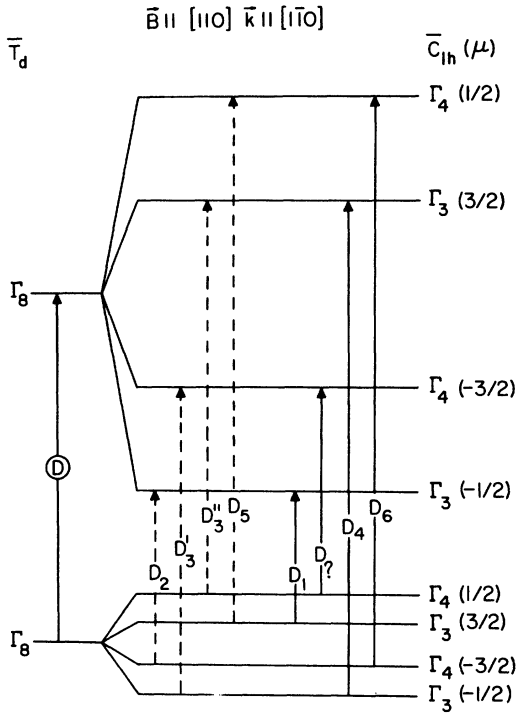

FIG. 25. Predicted energy-level and electric-dipole transition scheme for the Zeeman D components of boron in germanium with $\vec{B} \parallel [110]$ and $\vec{k} \parallel [1\bar{1}0]$.

is also the case for the transitions $\pm\frac{3}{2}\rightarrow\mp\frac{1}{2}$ and $\pm\frac{1}{2}\rightarrow\mp\frac{3}{2}$ for $E_\perp$. Such a result is inconsistent with the experimental evidence. Hence the choice of a positive value of v_D for $\vec{B}\parallel\langle 100\rangle$ is consistent with the observations for $\vec{B}\parallel\langle 110\rangle$.

From Fig. 25, and the counterparts of Eqs. (7) for the excited state of the D line, it is seen that the energy spacing of D_1 and D_5 gives a direct measure of g_2^D. Using the linear parameters in Table VII, it is found that $g_2^D = 2.75\pm 0.08$, which is in fair agreement with the value given in Table VIII. In addition, the energy spacings of either D_1 and D_2 or D_5 and D_6 should give a value for g_2'. The average obtained for g_2' from these two spacings is 0.78 ± 0.33. The numerical agreement between this value of g_2' and that given in Table VIII is fortuitous in view of the error. This error spans the two values of g_2' obtained from the two spacings mentioned above. If D_3 is taken in conjunction with any of the other components, the combination of g factors obtained is totally different from that expected. This is further evidence that D_3 is a composite of D_3' and D_3''.

Rather than using the a values of Table VII to determine the g factors, the g factors can be used to predict the a values. When this is done the results given in Table X are obtained. The errors indicated in the table are due to those in g_2' and g_2^D of Table VIII; additional error will result if the measured values of p' and p^D were used rather than the idealized value of $-\frac{9}{4}$. The agreement between the predictions of Table X and the data of Table VIII is good except for D_1 and D_3. For the latter, very little agreement is expected as this component is believed to be composed of D_3' and D_3''. In the case of D_1, the presence of the unobserved component $D_?$ (see Figs. 25 and 26) may produce some influence on its peak position.

In the idealized case, the predicted relative intensities for the C line, again taken to be a $\Gamma_8\rightarrow\Gamma_7$ transition, are relatively simple if the quadratic part is ignored. For $E_\parallel$, the intensities are in the approximate ratio $\pm\frac{3}{2}\rightarrow\pm\frac{1}{2}:\pm\frac{1}{2}\rightarrow\mp\frac{1}{2}: :0.44:0.06$, while for $E_\perp$ they are in the ratio $\pm\frac{3}{2}\rightarrow\mp\frac{1}{2}$ $\pm\frac{1}{2}\rightarrow\pm\frac{1}{2}: :0.01:0.49$. A detailed comparison has not been made between these results and the experimental data since very little of the latter is available. However, just as is the case for both $\langle 100\rangle$ and $\langle 111\rangle$, the Zeeman patterns of Figs. 19 and 20 are simple, although for the present orientation of $\vec{B}$ the C components are relatively broad. This may be due to the growth of the weak transitions under the quadratic effects predicted by BR and those arising from mixing effects.

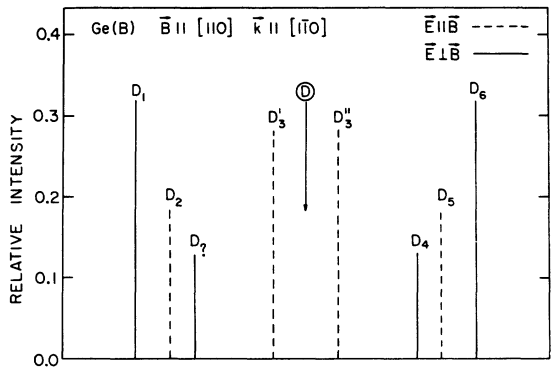

FIG. 26. Predicted relative intensities and linear shifts of the Zeeman D components of boron in germanium with $\vec{B}\parallel[110]$ and $\vec{k}\parallel[1\bar{1}0]$. A change to the right on the energy scale corresponds to an increase in energy.

C. $\vec{B}\parallel\langle 111\rangle$

As already pointed out, the interpretation given above for $\vec{B}\parallel\langle 100\rangle$ determines the parameters which govern the intensities of the Zeeman components and the linear splitting of the energy states for $\vec{B}\parallel\langle 111\rangle$. According to Eqs. (36a) and (36b) of BR, for $p'=-\frac{9}{4}$, the linear splitting of the Γ_8 ground state is given by

TABLE IX. Relative intensities predicted for the Zeeman components of the D line of boron impurity in germanium for $\vec{B}\parallel[110]$ and $\vec{k}\parallel[1\bar{1}0]$.[a]

Polarization	Component	Relative intensity
$E_\parallel$	$\pm\frac{3}{2}\rightarrow\pm\frac{1}{2}$	$\frac{1}{4}(1-u_D)+0.056u_D-0.236v_D=0.184$
	$\pm\frac{3}{2}\rightarrow\mp\frac{3}{2}$	$0.123u_D=0.012$
	$\pm\frac{1}{2}\rightarrow\pm\frac{3}{2}$	$\frac{1}{4}(1-u_D)+0.056u_D+0.236v_D=0.278$
	$\pm\frac{1}{2}\rightarrow\mp\frac{1}{2}$	$0.265u_D=0.027$
$E_\perp$	$\pm\frac{3}{2}\rightarrow\pm\frac{3}{2}$	$0.027(1-u_D)=0.024$
	$\pm\frac{3}{2}\rightarrow\mp\frac{1}{2}$	$0.223(1-u_D)+\frac{1}{4}u_D+0.473v_D=0.320$
	$\pm\frac{1}{2}\rightarrow\pm\frac{1}{2}$	$0.027(1-u_D)=0.024$
	$\pm\frac{1}{2}\rightarrow\mp\frac{3}{2}$	$0.223(1-u_D)+\frac{1}{4}u_D-0.473v_D=0.131$

[a]The results given are for the idealized case where $p'=p^D=-\frac{9}{4}$. Values of 0.1 and 0.2 have been used for u_D and v_D, respectively.

TABLE X. Predicted values of the a parameters of the D components of boron in germanium for $\vec{B}\parallel\langle 110\rangle$.[a]

Component	a (meV/kG) $\times 10^2$
D_1	−1.83
D_2	−1.45
$D_?$	−1.15
D_3'	−0.33
D_3''	+0.33
D_4	+1.15
D_5	+1.45
D_6	+1.83

[a]The parameter a determines the linear part of the Zeeman effect. An error of ± 0.06 in the units shown holds for each value given. The values correspond to the scheme given in Fig. 25.

$$E'_{\pm 3/2} = \pm\left[\left(\tfrac{3}{2}p' + \tfrac{23}{8}\right)^2 + \tfrac{1}{2}\right]^{1/2} \mu_B B g'_2$$
$$= \pm (\sqrt{3}/2)\, \mu_B B g'_2 , \qquad (8)$$
$$E'_{\pm 1/2} = \pm \left(\tfrac{1}{2}p' + \tfrac{13}{8}\right) \mu_B B g'_2 = \pm \tfrac{1}{2} \mu_B B g'_2 .$$

Similar expressions are obtained for the excited state of the D line in the idealized case. With this information an energy-level diagram can be constructed to scale for these two states. In addition, the relative intensities of the allowed transitions can be estimated using p' and p^D and the values of v_D and u_D arrived at earlier. In this manner, a prediction of the expected Zeeman pattern for the D line, excluding quadratic effects, can be readily obtained. Such a result is shown in Fig. 27. However, in this figure the actual values listed in Table VIII have been used in the construction. Very little change occurs in going from the idealized case described above to that shown in Fig. 27. The splittings corresponding to the expressions in Eqs. (8) become

$$E'_{\pm 3/2} = \pm (0.833^{+0.051}_{-0.044})\, \mu_B B g'_2 ,$$
$$E'_{\pm 1/2} = \pm (0.52 \pm 0.03)\, \mu_B B g'_2 ,$$
$$E^D_{\pm 3/2} = \pm (0.849 \pm 0.008)\, \mu_B B g^D_2 , \qquad (9)$$
$$E^D_{\pm 1/2} = \pm (0.510 \pm 0.005)\, \mu_B B g^D_2 .$$

The relative intensities calculated from the results

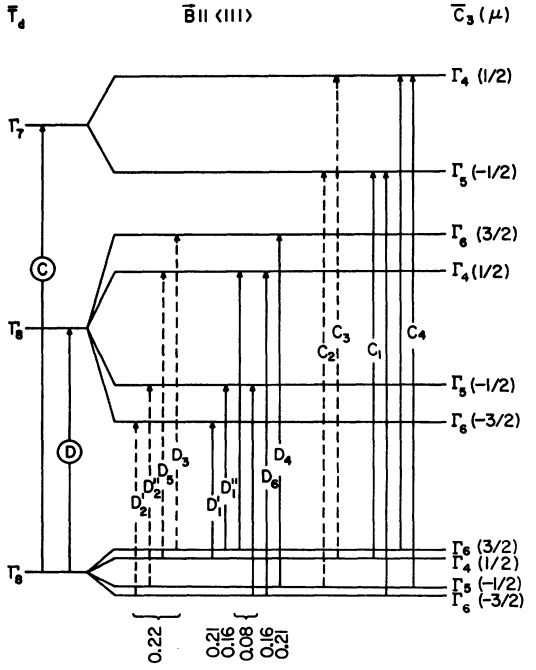

FIG. 27. Predicted energy-level and electric-dipole transition scheme for the Zeeman C and D components of boron in germanium with $\vec{B} \parallel \langle 111 \rangle$. The C line is assumed to be a $\Gamma_8 \rightarrow \Gamma_7$ transition. The predicted relative intensities are shown under the transitions.

TABLE XI. Relative intensities predicted for the Zeeman components of the D line of boron impurity in germanium for $\vec{B} \parallel \langle 111 \rangle$.[a]

Polarization	Component	Relative intensity
$E_\parallel$	$\pm\frac{3}{2} \rightarrow \pm\frac{3}{2}$	$\frac{1}{4}(1-u_D) = 0.225$
	$\pm\frac{3}{2} \rightarrow \mp\frac{3}{2}$	$\frac{1}{2}u_D = 0.050$
	$\pm\frac{1}{2} \rightarrow \pm\frac{1}{2}$	$\frac{1}{4}(1-u_D) = 0.225$
$E_\perp$	$\pm\frac{3}{2} \rightarrow \mp\frac{1}{2}$	0.157 ± 0.010
	$\pm\frac{1}{2} \rightarrow \pm\frac{3}{2}$	0.027 ± 0.001
	$\pm\frac{1}{2} \rightarrow \mp\frac{3}{2}$	0.211 ± 0.001
	$\mp\frac{1}{2} \rightarrow \pm\frac{1}{2}$	$\frac{1}{4}u_D = 0.025$
	$\mp\frac{3}{2} \rightarrow \mp\frac{1}{2}$	0.080 ± 0.010

[a]The values of p' and p^D given in Table VIII have been used to obtain the results for $E_\perp$, while for $E_\parallel$, p' and p^D have been taken to be $-\frac{9}{4}$. The values of u_D and v_D used are 0.1 and 0.2, respectively. No errors have been included in the values of u_D and v_D; the errors given are due to the errors in p' and p^D.

in Tables XIII A and XIII B of BR are given in Table XI. The values of u_D and v_D used to calculate these intensities were 0.1 and 0.2, respectively. No estimate has been made of the errors in these quantities; the errors given in Table XI reflect only the errors in p' and p^D. For $E_\parallel$, very little change occurs in the relative intensities if small deviations from $p' = p^D = -\frac{9}{4}$ are made. In view of this and the simplicity of the expressions for the relative intensities, only the idealized case is given for $E_\parallel$. For $E_\perp$, the two transitions, $\pm\frac{3}{2} \rightarrow \mp\frac{1}{2}$ and $\mp\frac{3}{2} \rightarrow \mp\frac{1}{2}$, depend on p' and not p^D and vice versa for the transitions $\pm\frac{1}{2} \rightarrow \pm\frac{3}{2}$ and $\pm\frac{1}{2} \rightarrow \mp\frac{3}{2}$. Hence, the relative intensities of the components within a given pair can be adjusted independent of those of the other pair. For sake of clarity, the very weak transitions $\pm\frac{3}{2} \rightarrow \mp\frac{3}{2}$, $\pm\frac{1}{2} \rightarrow \pm\frac{3}{2}$, and $\mp\frac{1}{2} \rightarrow \pm\frac{1}{2}$ have been omitted from Fig. 27. The relative intensities shown under the transitions in this figure are those of Table XI.

It is seen that four components of equal intensity are expected for $E_\parallel$. These should occur in pairs, each pair symmetrically disposed about the original line such that the spacing between the two inner components is about three times that of the spacing of each pair. In Fig. 14, only three $E_\parallel$ components are observed. Such a result could be obtained from the predictions of Fig. 27, if the transitions labeled D'_2 and D''_2 undergo quadratic shifts such that the energy of D'_2 increases relative to that given by the linear term only, while the energy of D''_2 is simultaneously decreased and brought into coincidence with D'_2. In this way D_2 would be a combination of D'_2 and D''_2. Such effects would also be experienced by D_3 and D_5. If the labeling of the transitions designated by D_3 and D_5 in Fig. 27 were interchanged then the same quadratic shifts which bring D'_2 and D''_2 into coincidence would cause D_3 and D_5

to move further apart than expected from Fig. 27. However, the results of the analysis of the data for the D line as given in Figs. 15 and 16 and Table VI predict that the linear shift of D_3 is greater than that of D_5; this is the reason for the labeling given for these components in Fig. 27. Hence, if D_3 is to be of lower energy than D_5 at high fields, there must be a strong repulsive quadratic effect depressing the energy of the excited $+\frac{3}{2}$ sublevel of the D line.

The energy scheme given in Fig. 27 can be used along with the results in Table VI to give information about the g factors. For example, the linear spacing of D_3 and D_2 should be proportional to $(g_2^D - g_2')$ if the average value of the energies of D_2' and D_2'' is used for that of D_2 and if in Eqs. (9) the numerical factor in $E'_{\pm 3/2}$ is taken equal to that in $E^D_{\pm 3/2}$ and the numerical factor in $E'_{\pm 1/2}$ taken equal to that in $E^D_{\pm 1/2}$. In this way it is estimated[57] that $g_2^D - g_2' = 3.62 \pm 0.36$, where the errors in $E'_{\pm 3/2}$ and $E'_{\pm 1/2}$ have been used. This is to be compared with the value of 2.33 ± 0.15 obtained from Table VIII. If the intercept D_3^{MIN} of Fig. 16 is used to find $(g_2^D - g_2')$ instead of the value of a for D_3 given in Table VI, than a value of ~ 3.2 is found for the difference of these two g factors. If the energy spacing between D_5 and D_2 is used, similar, and equally unsatisfactory, results are obtained for $(g_2^D - g_2')$.

The quadratic shifts invoked above to coalesce D_2' and D_2'' into D_2 for $E_\parallel$ need not exactly superimpose D_1' and D_1'' to give D_1 for $E_\perp$. Hence D_1 could be broader than D_2 as is observed experimentally (see Fig. 14). Again, as for D_3 and D_5, it is the crossing of D_4 and D_6 in Figs. 15 and 16 which causes D_4 rather than D_6 to be attributed to the transition $-\frac{1}{2} \rightarrow +\frac{3}{2}$, the crossing originating from the same strong repulsion of the $+\frac{3}{2}$ excited sublevel that is postulated to bring about the crossing of D_3 and D_5. Using D_4 and the average energy of D_1' and D_1'' for that of D_1, it is possible to determine a combination of g_2^D and g_2'. It is found that $(1.28 \pm 0.10) g_2^D + g_2' = 4.38 \pm 0.23$; this value is to be compared with the value of 4.76 ± 0.20 obtained for the g factors given in Table VIII. Unlike the result obtained from D_2 and D_3, the agreement obtained is reasonable. If the value for D_4^{MIN} (see Fig. 16) is used instead of the value of a for D_4 in Table VI, the value calculated for $(1.28 \pm 0.10) g_2^D + g_2'$ falls below 4.38 and the agreement becomes poor. The results suggest that the fit given in Fig. 16 for D_4 is good while that for D_3 is not. This is substantiated by the prediction in Fig. 27 that D_4 should have a larger energy than D_3 in contradiction to the results of the fits of Fig. 16 listed in Table VI. In fact, the energy spacing of D_3 and D_4 should give a direct measure of g_2'. If the results in Table VI are used in this way to find g_2', a negative value results, although the error is large enough to enable the g_2' determined to become positive; even then, however, the value of g_2' is much too small. Similar difficulties arise if the spacing of D_4 and D_5 is used to find g_2' although the value of g_2' found in this case is positive.

If we proceed as was done for $\vec{B} \parallel \langle 110 \rangle$ and estimate the a's for the different D components using Eqs. (9), the predictions obtained are those given in Table XII. These results, when compared with those of Table VI, suggest that D_1 and D_1'' are the same component; this we believe to be a fortuitous agreement as is that for D_4. If the interpretation that D_1 is the superposition of D_1' and D_1'', then $a(D_1)$ is predicted to be -1.53×10^{-2} meV/kG, which is still in reasonable agreement with the data for D_1 as may be appreciated from Fig. 16. In fact, except for D_2, all the predictions can be readily matched to the data. For D_2, interpreted to be the superposition of D_2' and D_2'', a value of -0.92×10^{-2} meV/kG is predicted for the intercept in Fig. 16; this is in poor agreement with the data and is not understood.

With regard to the predicted relative intensities of the D components, it can be seen from Fig. 27 that these should be in the proportion $D_1 : D_2 : D_3 : D_4 : D_5 : D_6 : : 0.37 : 0.44 : 0.22 : 0.21 : 0.22 : 0.16$. The agreement with the experimental results is reasonable except for the strengths of D_3 and D_5 which are larger relative to the other components than predicted. However, if the mixing effects which are postulated to account for the large shifts in D_3 and D_4 are real, then the relative intensities could be quite different from those expected, although such effects should be most noticeable in D_3 and D_4 and not D_3 and D_5. It may be this effect which is suppressing the two $E_\perp$ transitions, $\mp\frac{3}{2} \rightarrow \mp\frac{1}{2}$, whose intensities (see Fig. 27) should be large enough to be observed and whose energies

TABLE XII. Predicted values of the a parameters of the D components of boron in germanium for $\vec{B} \parallel \langle 111 \rangle$.[a]

Component	a (meV/kG) $\times 10^2$
D_1'	−1.76
D_1''	−1.29
D_2'	−1.15
D_2''	−0.68
D_3	1.15
D_4	1.76
D_5	0.68
D_6	1.29

[a]No errors have been estimated for these predictions. The labeling of the components corresponds to that given in Fig. 27.

should fall between those of D_1 and D_4. In fact, if this is not so, it is difficult to reconcile the absence of these two transitions with the predictions, since only a small decrease in their relative intensities is obtained when u_D is taken smaller than 0.1. If v_D is taken to be smaller than 0.2 these two unobserved transitions are reduced but not significantly, while conflict with the $\vec{B} \parallel \langle 100 \rangle$ interpretation would arise. It is probable that $u_D < 0.1$ since the two $E_\parallel$ transitions, $\pm\frac{3}{2} \rightarrow \mp\frac{3}{2}$, would then be further suppressed. A value of $u_D = 0.05$ would be more compatible with the observations than $u_D = 0.1$.

As was the case for $\vec{B} \parallel \langle 100 \rangle$, the C line for $\vec{B} \parallel \langle 111 \rangle$ exhibits a simple Zeeman pattern. In Fig. 27 is shown the prediction for the linear Zeeman effect of the C line for $\vec{B} \parallel \langle 111 \rangle$ as obtained from the results for $\vec{B} \parallel \langle 100 \rangle$. The relative intensities of the components can be estimated from the results given for a $\Gamma_8 \rightarrow \Gamma_7$ transition shown in Tables XIII A and XIII B of BR. It is predicted that the two components C_2 and C_3 for $E_\parallel$ should have the same intensities; this is not borne out by the experimental results (see Figs. 13 and 14). For $E_\perp$, three pairs of components are allowed, the intensities within each pair being equal. The transitions $\pm\frac{3}{2} \rightarrow \mp\frac{1}{2}$ and $\mp\frac{3}{2} \rightarrow \mp\frac{1}{2}$ depend upon p'. If the value of this quantity obtained from the $\langle 100 \rangle$ data is used, then these two pairs of transitions have the relative intensities 0.010 and 0.365, respectively. The relative intensities of each component in the third pair of transitions, viz., $\mp\frac{1}{2} \rightarrow \pm\frac{1}{2}$, is independent of p' and is simply $\frac{1}{8}$. If it is assumed that the pair of very weak transitions is missing then the scheme shown in Fig. 27 is obtained. However, in order to justify the disagreement between the observed and predicted intensities, it must be assumed that there are substantial mixing effects which drastically distort the relative intensities from those predicted just as was the case for $\vec{B} \parallel \langle 100 \rangle$. The fact that the straight lines in Fig. 17 fitted to C_1 and C_2 are not parallel to those fitted to C_3 and C_4 gives a good indication that there are quadratic effects over and above those considered in the theory of BR.

From the energy spacings of C_1 and C_3, and C_2 and C_4 a value of $g^C_{(7)} = 2.06 \pm 0.14$ is obtained for boron. This is to be compared with the value given in Table VIII. The fact that these two values are different could be due to a linear term introduced via the mixing. Since the mixing for $\vec{B} \parallel \langle 100 \rangle$ appears to be smaller than for $\vec{B} \parallel \langle 111 \rangle$, the former value should be more correct even though the latter agrees closely with that calculated by LCW (see Table VIII). The energy spacings of C_1 and C_2, and C_3 and C_4, should be a measure of g'_2. However, since C_1 is broader than the other lines, possibly because of the presence of the transition $-\frac{3}{2} \rightarrow -\frac{1}{2}$, only the C_3 to C_4 spacing was used to find g'_2. The value thus obtained was 0.42 ± 0.18, which is substantially lower than the value given in Table VIII. It is not clear why this is so since the ground state should be relatively free of any mixing.

The G line for $\vec{B} \parallel \langle 111 \rangle$ exhibits even more asymmetry than it did for $\vec{B} \parallel \langle 100 \rangle$. Not only are the intensities of the $E_\perp$ components totally different, but so are those of the $E_\parallel$ components. Since the values of p for different Γ_8 states seem to be close to the idealized value, it is not unreasonable to expect that p^G will also be close to $-\frac{9}{4}$. In fact the calculation of LCW (see footnote to Table VIII) bears this out. Although the signs of their g factors are different from those deduced here for $\vec{B} \parallel \langle 100 \rangle$, this will not affect the sign of p^G. The number of G components expected in this case for $\vec{B} \parallel \langle 111 \rangle$ will be the same as for the D line, viz., four for each polarization, whereas for $\vec{B} \parallel \langle 100 \rangle$ only two relatively strong $E_\parallel$ components are expected. Hence, if an argument similar to that used for the G line in the case of $\vec{B} \parallel \langle 100 \rangle$ were followed for $\vec{B} \parallel \langle 111 \rangle$, it might be possible to have several components superimpose not only for $E_\perp$ but also for $E_\parallel$.

VI. CONCLUSIONS

In general, it is clear that the observed Zeeman patterns for the D line are qualitatively in good agreement with those predicted. Of the three orientations studied, the least well understood is the case of $\vec{B} \parallel \langle 111 \rangle$ mainly, it is believed, because the splittings, quadratic effects, and relative intensities have conspired to make it difficult to obtain well-resolved components except at large fields. For the C line, some agreement is obtained between theory and experiment, the principal discrepancies being found in the comparison of relative intensities. For the G line very little understanding has been obtained.

Since boron has the most effective-mass-like ground state of all the group-III impurities, it is expected that the calculated g factors should be closer to those measured for boron than for thallium. The value of -1.30 obtained by Suzuki *et al.*[29] for $g'_{1/2}$ is in better agreement with the experimental results than is that obtained by LCW (see Tables I and VIII) but is closer to the result for thallium than to that for boron. However, the large error in $g'_{1/2}$ for thallium precludes this from being distinguishable from the corresponding value for boron. This is not the case, though, for $g'_{3/2}$. It is clear from Table VIII that $g'_{3/2}$ is substantially larger for thallium than for boron and close to the value calculated by LCW. This latter agreement may be fortuitous since in the calculations of Suzuki *et al.*, $g'_{3/2}$ was found to be very

sensitive to the value chosen for the valence-band parameter κ.[29] In Table I are shown these latter results; a value of -0.19 is obtained for $g'_{3/2}$ if κ is taken to be 3.9, while $g'_{3/2}$ is found to be 0.35 if κ is chosen as 3.29. The most recent determination of κ is that by Hensel and Suzuki[50]; they find that κ is 3.41 ± 0.03. If $g'_{3/2}$ were recalculated using this latter value of κ (which lies between the two different values chosen by Suzuki *et al.*) it might be expected to be positive, but whether or not it could be as small as 0.03, the value obtained for boron from the D line (see Table VIII) or even as small as 0.08, the value obtained from the C line (see Sec. V A), is not clear. Nor is it clear how $g'_{1/2}$ is affected using this value of κ. It might be noted that the g factors calculated by Bir *et al.*[28] show no agreement with the experiment.

The excited state of the D line has principal g factors that are, experimentally, essentially the same for boron and thallium (see Table VIII), although the error in $g^D_{3/2}$ for thallium is considerable. This verifies what has been observed previously, viz., that the excited states of the group-III impurities in germanium are species independent.[20] The agreement between the calculated value of $g^D_{1/2}$ and that obtained experimentally is not as good as might be expected for a truly effective-mass-like excited state. However, good agreement is obtained for $g^D_{3/2}$. Even though the signs of the experimental and calculated values of $g^D_{3/2}$ are opposite, their magnitudes are very small and hence there could be sufficient error in the calculated value to bring about agreement.

The experimental results given in Table VIII for $g^C_{(7)}$ for boron and thallium do not quite overlap. If the value of 2.14 discussed in Sec. V A is taken for $g^C_{(7)}$ of thallium better agreement is obtained, assuming similar errors. The agreement between the experimental and calculated values is not unreasonable since the C components may be subject to mixing effects.

The relative intensities for the observed D components are consistent with values of 0.05 and 0.2 for u_D and v_D, respectively. The ratios obtained with this choice of parameters for $\vec{B} \parallel \langle 100 \rangle$ are $D_1 : D_2 : D_3 : D_4 : D_5 : D_6 : D_7 : D_8 :$ $: 0.29 : 0.15 : 0.19 : 0.35 : 0.35 : 0.19 : 0.15 : 0.29$. The four weak $E_\perp$ transitions have relative intensities of 0.01. The only qualitative difference between the predicted intensities and those observed is that D_7 is somewhat larger than is expected; this has been attributed to a mixing effect. In addition to this, though, the intensity of each component is directly proportional to its energy, an effect which is not negligible in the present measurements at the highest fields used; this has not been taken into account.

Substantial agreement has been obtained between the experimental results for the D line with $\vec{B} \parallel [110]$, $\vec{k} \parallel [1\bar{1}0]$, and the predictions for this orientation based on the parameters determined from the interpretation of the $\langle 100 \rangle$ data. This agreement is found for both the g factors and the intensities and hence appears to verify the $\langle 100 \rangle$ interpretation even to the sign of v_D. It would be interesting to study the other direction of propagation of radiation, viz., $\vec{k} \parallel [001]$, considered by BR; this should provide information about some of the transitions that are unobserved for $\vec{k} \parallel [1\bar{1}0]$.

The agreement between predictions and experiment for $\vec{B} \parallel \langle 111 \rangle$ is not as satisfactory as in the other two cases. Some success has been achieved but, in order to obtain this, it has been necessary to invoke substantial quadratic effects due to mixing of states. These effects are not strikingly evident for the other two orientations. Within the framework of the theory of BR, the intensities for $\vec{B} \parallel \langle 110 \rangle$ are expected to be dependent upon $|\vec{B}|$ via quadratic effects, but even this has not distorted the Zeeman pattern sufficiently to prevent an apparently quite clear interpretation to be obtained in this case. Hence, the assumptions necessary to understand, at least in part, the $\langle 111 \rangle$ case are not as convincing as one would like. It would appear that a better understanding of the effect for $\vec{B} \parallel \langle 111 \rangle$ must await experiments carried out under higher resolution than that achieved here in order to determine better the linear splitting parameters and the relative intensities.

For all three orientations of $\vec{B}$, the Zeeman pattern of the C line was found to be quite simple. The results have been interpreted with partial success in terms of a $\Gamma_8 \rightarrow \Gamma_7$ transition. This is contrary to the results of piezospectroscopic studies of group-III impurities[26,27] in which at least four C components are observed for a force applied along a $\langle 100 \rangle$ direction. A $\Gamma_8 \rightarrow \Gamma_7$ transition can split into two components at most under such a perturbation. However, a detailed understanding of the behavior of the C line due to strain has not been obtained.

The G line has not been convincingly interpreted. This is surprising because it is felt that, since its final state is much more isolated than all other excited states, the perturbation approach of BR would be most applicable. In addition, the quadratic effects for this state should be smaller than, for example, those of the final state of the D line since the dimensions of the Bohr orbits of the states are different (see Figs. 6 and 7 of Ref. 21). That these effects should be so large as to completely mask the linear effects is difficult to understand. However, if this postulate is correct, it can be verified by experiments at lower magnetic fields and under higher resolution. A piezospectroscopic study of this line has yet to be made,

such an investigation might unambiguously establish that the transition is, in reality, a $\Gamma_8 - \Gamma_8$ excitation.

Finally, it should be noted that very little information has been extracted regarding the q factors of the various states. If all the observed quadratic effects are attributed to the excited states more information can be obtained but, since all the acceptor states including the ground state have large spatial dimensions, this would appear to be a poor approximation.

ACKNOWLEDGMENTS

The authors wish to thank Dr. A. K. Bhattacharjee and Professor S. Rodriguez for many stimulating and informative discussions on the present work. They also wish to thank N. R. Butler for the computer program used in analyzing the experimental data and S. R. Thomas for a number of discussions relevant to the construction of the cooled bolometer that was used as the detector. In addition, we wish to thank Dr. A. Krauss and Professor J. K. Furdyna for the use of their electrodepositing unit to fabricate a light pipe used with the detector. Finally, thanks are due to D. Bilderback and Professor R. Colella for the use of the x-ray diffraction unit to check the orientation of the germanium samples.

*Work supported by the National Science Foundation, Advanced Research Projects Agency, and the Purdue Research Foundation.

†Permanent address: Department of Physics, Institut Teknologi Bandung, Bandung, Indonesia. Leave sponsored by the Agency for International Development.

[1]P. Fisher and A. K. Ramdas, in *Physics of the Solid State*, edited by S. Balakrishna, M. Krishnamurthi, and B. Ramachandra Rao (Academic, New York, 1969), p. 149.

[2]W. Kohn, in *Solid State Physics*, edited by F. Seitz and D. Turnbull (Academic, New York, 1957), Vol. 5, p. 257.

[3]J. H. Reuszer and P. Fisher, Phys. Rev. **135**, A1125 (1964).

[4]R. L. Aggarwal and A. K. Ramdas, Phys. Rev. **137**, A602 (1965).

[5]R. A. Faulkner, Phys. Rev. **184**, 713 (1969).

[6]W. H. Kleiner and W. E. Krag, Phys. Rev. Lett. **25**, 1490 (1970).

[7]N. R. Butler, P. Fisher, and A. K. Ramdas (private communication).

[8]J. H. Reuszer and P. Fisher, Phys. Rev. **140**, A245 (1965). Phys. Rev. **165**, 909 (1968).

[9]R. L. Aggarwal and A. K. Ramdas, Phys. Rev. **140**, A1246 (1965).

[10]V. J. Tekippe, H. R. Chandrasekhar, P. Fisher, and A. K. Ramdas, Phys. Rev. B **6**, 2348 (1972).

[11]W. E. Krag, W. H. Kleiner, and H. J. Zeiger, in *Proceedings of the Tenth International Conference on the Physics of Semiconductors, Cambridge, Mass., 1970*, edited by S. P. Keller, J. C. Hensel, and F. Stern (U.S.A.E.C., Division of Technical Information, Washington, D.C., 1970), p. 271.

[12]P. Fisher and H. Y. Fan, J. Phys. Chem. Solids **8**, 270 (1959).

[13]W. S. Boyle, J. Phys. Chem. Solids **8**, 321 (1959).

[14]B. Lax, L. M. Roth, and S. Zwerdling, J. Phys. Chem. Solids **8**, 311 (1959).

[15]S. Zwerdling, K. J. Button, and B. Lax, Phys. Rev. **118**, 975 (1960).

[16]R. R. Haering, Can. J. Phys. **36**, 1161 (1958).

[17]W. S. Boyle and R. E. Howard, J. Phys. Chem. Solids **19**, 181 (1961).

[18]Y. Nisida and K. Horii, J. Phys. Soc. Jap. **31**, 776 (1971); K. Horii and Y. Nisida, J. Phys. Soc. Jap. **31**, 783 (1971).

[19]B. Pajot, F. Merlet, G. Taravella, and Ph. Arcas, Can. J. Phys. **50**, 1106 (1972); B. Pajot, F. Merlet, and G. Taravella, Can. J. Phys. **50**, 2186 (1972).

[20]R. L. Jones and P. Fisher, J. Phys. Chem. Solids **26**, 1125 (1965).

[21]K. S. Mendelson and H. M. James, J. Phys. Chem. Solids **25**, 729 (1964).

[22]A. Onton, P. Fisher, and A. K. Ramdas, Phys. Rev. **163**, 686 (1967).

[23]D. Schechter, J. Phys. Chem. Solids **23**, 237 (1962).

[24]K. S. Mendelson and D. R. Schultz, Phys. Status Solidi **31**, 59 (1969).

[25]H. R. Chandrasekhar, P. Fisher, A. K. Ramdas, and S. Rodriguez, Phys. Lett. A **41**, 137 (1972).

[26]R. L. Jones and P. Fisher, Phys. Rev. B **2**, 2016 (1970).

[27]D. H. Dickey and J. O. Dimmock, J. Phys. Chem. Solids **28**, 529 (1967).

[28]G. L. Bir, E. I. Butikov, and G. E. Pikus, J. Phys. Chem. Solids **24**, 1467 (1963).

[29]K. Suzuki, M. Okazaki, and H. Hasegawa, J. Phys. Soc. Jap. **19**, 930 (1964).

[30]P. Fisher and H. Y. Fan, Phys. Rev. Lett. **2**, 456 (1959).

[31]R. Kaplan (private communication) has made longitudinal Zeeman-effect measurements (Faraday configuration) on the excitation spectra of boron and thallium impurities in germanium. Similar measurements have also been made recently by F. Merlet and B. Pajot (private communication) for boron in silicon.

[32]P. J. Lin-Chung and R. F. Wallis, J. Phys. Chem. Solids **30**, 1453 (1969). In the remainder of the text this reference will be designated by LCW.

[33]A. K. Bhattacharjee and S. Rodriguez, Phys. Rev. B **6**, 3836 (1972). In the remainder of the text this reference will be designated by BR.

[34]H. P. Soepangkat, P. Fisher, and S. Rodriguez, Phys. Lett. A **39**, 379 (1972).

[35]H. P. Soepangkat, A. K. Bhattacharjee, P. Fisher, and S. Rodriguez, in *Proceedings of the Eleventh International Conference on the Physics of Semiconductors, Warsaw, Poland, 1972* (PWN-Polish Scientific Publishers, Warsaw, 1972), p. 1037.

[36]H. P. Soepangkat, Ph.D. thesis (Purdue University, 1972) (unpublished).

[37]Manufactured by the Perkin-Elmer Corp., Norwalk, Conn. 06852.

[38]We are indebted to Dr. D. Dickey of Lincoln Laboratory for selecting this element from a germanium ingot grown at Purdue University by Miss Louise Roth to Dr. Dickey's specifications.

[39]Manufactured by Texas Instruments, Inc., 3609 Buffalo Speedway, Houston 6, Tex.

[40]S. Zwerdling, R. A. Smith, and J. P. Theriault, Infrared Phys. 8, 271 (1968).

[41]Manufactured by General Electric Co., Minature Lamp Department, Nela Park, Cleveland, Ohio 44112.

[42]K. Nahari Rao, R. V. DeVore, and E. K. Plyler, J. Res. Natl. Bur. Stand. (U.S.) A **67**, 351 (1963).

[43]Manufactured by Varian, Analytical Instruments Div., 611 Hansen Way, Palo Alto, Calif. 94303.

[44]P. Fisher, W. H. Haak, E. J. Johnson, and A. K. Ramdas, in

Proceedings of the Eighth Symposium on the Art of Glass Blowing (The American Scientific Glass Blowers Society, Wilmington, Del., 1963), p. 136.
[45]R. D. Hancock and S. Edelman, Rev. Sci. Instrum. **27**, 1082 (1956); see also J. W. Edwards, Semicond. Prod. **6**, 30 (1963); Semicond. Prod. **6**, 34 (1963).
[46]Type *A* Preamplifier and Model HR-8 Lock-in Amplifier, Princeton Applied Research Corp., P. O. Box 565, Princeton, N.J.
[47]A. Onton, Ph.D. thesis (Purdue University, 1967) (unpublished).
[48]A. Savitsky and M. J. E. Golay, Anal. Chem. **36**, 1627 (1964).
[49]W. H. Kleiner, MIT Lincoln Laboratory, Quarterly Report, Solid State Research, November 1958, p. 54 (unpublished).
[50]J. C. Hensel and K. Suzuki, in Ref. 11, p. 541.
[51]J. J. Stickler, H. J. Zeiger, and G. S. Heller, Phys. Rev. **127**, 1077 (1962).
[52]S. Rodriguez, P. Fisher, and F. Barra, Phys. Rev. B **5**, 2219 (1972).
[53]A comparison of LCW's results for the D line and $E_{||}$ (see Fig. 2 of Ref. 32) and those given in Table II shows that the ratio of the intensities of the two pairs of D components for $E_{||}$ is about 6.74, thus giving $v_D \simeq \pm 3/8$. The ambiguity in the sign of v_D is due to the different transitions in Ref. 32 not being identified. A similar comparison for $E_\perp$ of the four D components of equal intensity gives $u_D \simeq 1/6$, a value which is compatible with the intensities of the remaining $E_\perp$ components and the above value of v_D. A comparison, in a like manner, of the G components in Fig. 2 of LCW gives the values for u_G and v_G. It should be noted that if the two weak G components for $E_\perp$ were of zero intensity then u_G and $|v_G|$ would be exactly 8/9 and 1/3, respectively.
[54]In reaching these conclusions, it was assumed that D_8 is of larger energy than D_7 although within the experimental error these appear to have the same linear Zeeman shift.
[55]It might be noted that the errors in these values of g_1^D and g_2^D are substantially smaller than those given in Table VIII. This simply reflects the fact that the most probable errors in this case are smaller than the difference between the average $E_\mu - E_{-\mu}$ and each individual $E_\mu - E_{-\mu}$.
[56]If this is a correct representation of the behavior of D_4, it is difficult to understand in view of the prominence of this component. The accuracy with which the energy of this component can be determined appears to preclude this possibility.
[57]In this calculation the quantities given in Eqs. (9) contain the values of p' and p^D. Since these each lie close to the idealized case it is assumed that the combination of g_2' and g_2^D obtained here and later are relatively independent of the values of p' and p^D.

PHYSICAL REVIEW B VOLUME 8, NUMBER 2 15 JULY 1973

Energy and Temperature Dependence of Low-Energy-Electron Diffraction from Xenon Single Crystals*

A. Ignatiev† and T. N. Rhodin
School of Applied and Engineering Physics, Cornell University, Ithaca, New York 14850
(Received 5 January 1973)

A complete set of intensity-energy spectra as a function of electron energy, crystal temperature, and incidence angle have been measured for the specular and the first-order nonspecular beams for the (111) xenon surface. The xenon single crystals were formed by epitaxial deposition onto a (100) iridium substrate and were of excellent order and purity. The character of the intensity-energy spectra indicated xenon to be a highly kinematic electron scattering material. Hence the formalism for kinematic scattering could be applied with confidence to the analysis of electron scattering in xenon and with specific reference to the surface dependence of the effective Debye temperature and to surface-layer thermal expansion.

I. INTRODUCTION

Since the inception of low-energy-electron diffraction (LEED) by Davisson and Germer in 1927,[1] it has been indicated that LEED would be able in principle to describe the atomic positions, electronic structure, and vibrational properties of surfaces of single crystals similarly to those of x-ray diffraction for the bulk. Complete analysis of a typical LEED spectra, however, has proved to be a formidable problem because of the occurrence of multiple scattering associated with the very strong interaction of the electrons with the atoms. Recently model calculations in which such events are considered in terms of formal scattering theory have shown good agreement with experiment. These computations are involved and time consuming using $\frac{1}{2}$–4 h of computer time on large computers.[2–4] Therefore, the application of such calculations to the solution of the surface structure and surface properties of specific electron scattering systems at the present time does not provide as yet a routine procedure for structure analysis.

One way of simplifying the problems of a complete multiple scattering analysis is to analyze the electron scattering data in the kinematic scattering formalism. This, however, leads to realistic results only for systems that truly exhibit kinematic features. For electron scattering from most crystalline solids such systems are not typical because